의학박사 학위논문

Role of miRNAs in chemo- and radio-sensitization of non-small cell lung cancer cell lines

비소세포함 세포주의 항암제 및 방사선 내성을 조절하는 miRNA에 대한 연구

2012 년 8 월

서울대하교 대학원

의과학과

규레시 레하나

비소세포함 세포주의 항암제 및 방사선 내성을 조절하는 miRNA 에 대한 연구

지도교수 박웅양

이 논문을 의학박사 학위논문으로 제출함

2012 년 6 월

서울대하교 대학원

의과학과

규레시 레하나

규레시 레하나의 의학 박사 학위논문을 인증함

2012 년 8 월

위 원 장 DoSyLee DoSyLee

부위원장 박웅양

위 원 장 예상규

위 원 장 안정혁

위 원 장 조정현

Role of miRNAs in chemo- and radio-sensitization of non-small cell lung cancer cell lines

by

Rehana Qureshi

A thesis Submitted to the Department of Biomedical Science in the Partial Fulfillment of the Requirements for the Degree of Doctor of Philosophy in Medical Sciences at the Seoul National University, College of Medicine

June 2012

Approved by thesis committee:

Professor Dong Suplee Chairman

Professor Woongyang Park Vice Chairman

Professor Jong-Kyu Lee

Professor Sung Hyuck Ahn

Professor Chang-Hyun Cho

ABSTRACT

Rehana Qureshi
Department of Biomedical Science
Seoul National University College of Medicine

Non-small cell lung cancer (NSCLC) is a remarkably heterogeneous disease and remains largely incurable due to resistance developed against the drugs and ionizing radiations. The activation of nuclear factor-kappa B1 (NFκB1) in cancer cells may confer resistance to ionizing radiation (IR). To enhance the therapeutic efficiency of IR in lung cancer, I screened for miRNAs that suppress NFκB1 and observed their effects on radio sensitivity in a human lung cancer cell line. From time series data of miRNA expression in γ-irradiated H1299 human lung cancer cells, I found that the expression of miR-9 was inversely correlated with that of NFκB1. Overexpression of miR-9 down-regulated the level of NFκB1 in H1299 cells, and the surviving fraction of γ-irradiated cells was decreased. Interestingly, let-7g also suppressed the expression of NFκB1, al- though there was no canonical

target site for let-7g in the NFκB1 3' untranslated region. From these results, I conclude that the expression of miR-9 and let-7g could enhance the efficiency of radiotherapy for lung cancer treatment through the inhibition of NFκB1.

Next, I wanted to expand the area of investigation to understand the mechanisms of resistance development. Hence, I studied the role of PRDM5 gene, whose precise function remained unclear till now. I found that it is highly expressed in the NSCLC. Knockdown of the PRDM5 reduced the growth of cancer cell as well as it leads to the radio and chemo sensitization of NSCLCs. I have shown a mechanism in which PRDM5 binds to the promoter of miR-135b, thereby leading to its suppression. This abrogation leads to high expression of HIF1α , which is a conserve target of miR-135b. Apart from this, overexpression of miR-135b attenuates the growth of tumor cell lines and sensitized them toward radiation and drugs. My finding demonstrates a new insight into the signaling cascades, which influence HIF1α in NSCLC as well as suggest that PRDM5 is a potential therapeutic target.

Student Number: 2009-31326

국문초록

레하나 큐레시
서울대학교 대학원 의과학과

비소세포성 폐암 (non-small cell lung cancer, NSCLC) 세포에서 nuclear factor-kappa B1(NFKB1)의 활성화는 전리방사선(ionizing radiation, IR)에 대한 저항성을 부여한다. 폐암에서 방사선치료 저항성에 대한 miRNA의 역할을 분석하기 위해 사람의 폐암세포인 H1299에 방사선을 준 후 시간흐름에 따른 miRNA의 발현양상을 확인하여 NFKB1을 억제하는 miRNAs를 선별하였다. 그 결과 miR-9의 발현이 NFKB1의 발현과 연관이 있는 것을 알 수 있었다. H1299 세포에서 miR-9에 의한 NFKB1의 단백질 번역 조절과 전리방사선 처리에 대한 세포생존률을 분석하였다. miR-9의 과발현에 의해 NFKB1의 단백질 번역이 감소하였으며, 전리방사선을 처리한 후에 세포생존률도 감소하였다. NFKB1의 3'-untranslated region (3'-UTR)에는 let-7g의 결합부위가 없음에도 불구하고 NFKB1의 단백질 번역을 억제할 수 있었다. 이러한 결과로부터 miR-9과 let-7g가 NFKB1을 단백질 번역을 억제하여 비소세포성폐암 세포주의 전리방사선에 대한 반응성을 증가시킨다는 것을 알 수 있었다.

PR domain containing 5 (PRDM5)는 전사인자 단백질로서 miRNA를 비롯한 여러 유전자의 발현을 억제한다. PRDM5를 감소시키면 종양세포의 성장이 줄고, 특히 비소세포성 폐암의 전리방사선 및 항암제에 대한 민감성을 증가시킬 수 있다. 전리방사선에 의해 발현이 증가한 PRDM5는 miR-135b의 promoter 부위에 붙어 발현을 억제하였다. 또한 miR-135b의 감소는 HIF1a의 단백질 번역의 증가를 유도하였다. 반대로 PRDM5를 억제하면 세포의 성장을 줄고, 항암제와 전리방사선에 대한 민감성이 증가하였다. 또한 miR-135b의 발현은 A549 및 H1299

비소세포성 폐암세포주의 성장을 억제하고 전리방사선 및 항암제 민감성을 증진시킬 수 있었다. PRDM5와 miR-135b 및 HIF1a의 상호작용은 폐암세포 조직 유전자발현 데이터베이스 및 NCI-60 종양세포주 유전자발현 데이터베이스에 대한 메타 분석에서 확인할 수 있었다. 이러한 결과로부터 PRDM5는 비소세포성 폐암의 치료에 있어서 우수한 치료표적이 될 수 있다는 것을 알 수 있었다.

학번: 2009-31326

Table of contents

Chapter I
miR-9 and let-7g enhance the sensitivity to ionizing radiation by suppression of NFkB1

List of figures I

List of Tables I

Chapter II

Role of PRDM5 and miR-135b in radio and chemo sensitization of NSCLC's

List of figures II

List of tables II

Chapter I

MiR-9 and let-7g enhance the sensitivity to ionizing radiation by suppression of NFkB1

ABSTRACT

The activation of nuclear factor-kappa B1 (NFkB1) in cancer cells may confer resistance to ionizing radiation (IR). To enhance the therapeutic efficiency of IR in lung cancer, I screened for miRNAs that suppress NFkB1 by considering time series data of miRNA expression in-irradiated H1299 human lung cancer cells. I found that the expression of miR-9 was inversely correlated with that of NFkB1. I checked the impact of over-expression of miR-9 on the level of NFkB1 in H1299 cells, followed by the surviving fraction analysis via MTT assay. Over-expression of miR-9 down-regulated the level of NFkB1 in H1299 cells, and the surviving fraction of γ-irradiated cells was decreased. Interestingly, let-7g also suppressed the expression of NFkB1, although there was no canonical target site for let-7g in the NFkB1 3' untranslated region. Together, I concluded that, the expression of miR-9 and let-7g could enhance the efficiency of radiotherapy for lung cancer treatment through the inhibition of NFkB1.

Keywords: ionizing radiation, let-7g, lung cancer, miR-9, NFkB1

INTRODUCTION

Upon exposure to ionizing radiations, a series of alterations occurs in the cells including transformation, cell cycle distress, mutations, sister-chromatid exchanges, chromosome aberrations, DNA repair, and apoptosis (Preston 2005; Amundson 2008). The impact of IR exposure in cells is determined by the cellular gene expression pattern (Amundson, Bittner et al. 2003). Among the IR-responsive genes, the activation of nuclear factor-kappa B1 (NFkB1) following genotoxic stress allows DNA damage repair and cell survival (Janssens, Tinel et al. 2005). The activation of NFkB1 in cancer cells may induce radioresistance, which frequently prevents successful treatment (Chen, Tao et al. 2002; Aggarwal, Vijayalekshmi et al. 2009).

NFkB1 suppression induces the sensitivity of cancer cells to apoptotic action of chemotherapeutic agents and radiation exposure (Li and Sethi 2010). Several NFkB1 inhibitors have been actively investigated as potential adjuvant therapeutics for lung cancer together with radiotherapy (Kunnumakkara, Diagaradjane et al. 2008). Radiosensitization induced by anti-inflammatory cytokines such as interleukin IL-4 and IL-10 in colorectal cancer was associated with NFkB1 inhibition (Voboril and Weberova-Voborilova 2007). miRNA (miRNA) are short 20-22 nucleotide entities which plays a significant role at the post-transcriptional gene regulation based on the 3' untranslated region (UTR) sequences. The alteration of miRNA expression upon IR may affect the gene regulation in the cellular

response to radiation exposure (Chaudhry, Kreger et al. 2010). It is important to find miRNAs targeting NFkB1 as a potential therapeutic approach to overcome radioresistance in cancer treatment.

Several studies have investigated the transcriptional regulation of mRNAs and miRNAs in γ-irradiated cells to understand cellular responses to IR (Park, Hwang et al. 2002; Weidhaas, Babar et al. 2007; Jeong, Wu et al. 2009). In this study, I screened the expression profiles of miRNA in γ-irradiated H1299 human lung cancer cell line to find miRNA targeting NFkB1. I found that miR-9 and let-7g could increase the sensitivity of H1299 cells to IR *in vitro*. Thus, I propose that the suppression of NFkB1 by miR-9 and let-7g may provide opportunities for both prevention and treatment of cancer.

MATERIALS AND METHODS

Cell culture and γ-irradiation

H1299 and A549 human lung cancer cell lines were maintained in RPMI 1640 medium supplemented with 10% fetal bovine serum, 100 U/mL penicillin, 100 μg/mL streptomycin, and 2 mM L-glutamine. The cultured cells were either exposed to 0-10 Gy of radiation using a 4-MV linear accelerator (Clinac 4/100, Varian, Palo Alto, CA, USA) or left irradiated as a negative control.

MiRNA microarray and statistical analysis

miRNAs were extracted using the mirVana miRNA isolation kit (Ambion, Austin, TX, USA) according to the manufacturer's protocols. Purified miRNAs were labeled using the mirVana miRNA Array Labeling Kit and coupled to the Cy5 Post-Labeling Reactive Dye (Amersham, GE Healthcare Bio-Sciences, Piscataway, NJ, USA). The labeled samples were washed and hybridized in duplicate to mirVana miRNA Bioarrays (Ambion) using the mirVana miRNA Bioarray Essentials Kit. Fluorescence intensities were processed and measured using the GeneChip scanner 3000 7G (Agilent Technologies, Santa Clara, CA, USA). The levels of miRNA hybridization were determined using GenePix Pro 6.0 software as recommended by the manufacturer. The background-adjusted intensity for each miRNA was subjected to a global variance stabilization normalization (VSN) procedure (Huber, von Heydebreck et al. 2002). The miRNAs targeting NFkB1were predicted using TargetScan, and Pearson's correlation coefficient was

calculated between the expression levels of miRNA and NFkB1 transcript (Sung, Wu et al. 2010) .

Constructs and transfection

The precursor of the hsa-miR-9 was amplified from the H1299 genomic DNA using the primers 5'-CCGGAATTC CCTCAACTCCACTCGTGTCC-3' and 5'-ATTGCGGCCGCTGGGACTGTG ACTCCTACCTG-3', and the resulting product was cloned into EcoR1/Not1 restricted pcDNA3 (Invitrogen, Carlsbad, CA, USA). The precursor of the has-miR-26b was amplified from the H1299 genomic DNA using the primers 5'CGGATGGGAATTGGAT ACAT3' and 5' AGCTACCCTGACCACTGCTG 3'cloned into PGEMT easy vector (Promega, Madison, WI, USA). The resulting product was subcloned into EcoR1/Not1 restricted pcDNA3.

The expression vector for hsa-let-7g was provided S-H. Jeong (Jeong, Wu et al. 2009), and the construct was transfected using FuGENE HD (Roche Applied Science, Mannheim, Germany) according to the manufacturer's protocols. Total RNA for real-time PCR, protein for western blot, and cells for MTT assay were collected after 48 hrs of transfection.

RNA preparation and quantitative real-time RT-PCR

Total RNA was extracted from cell lines using the TRIzol method according to the manufacturer's protocol (Kwak, Jeong et al. 2009). Total RNA was reverse transcribed to complementary DNA using

Superscript II reverse transcriptase (Invitrogen) and oligonucleotide primers. Quantitative RT–PCR for genes was performed in a reaction mixture containing complementary DNA, SYBR Premix Ex Taq (Takara Bio Inc., Shiga, Japan), and primers for each gene. Quantitation of miRNAs was carried out using TaqMan miRNA assays (Applied Biosystems, Foster City, CA, USA). The PCR amplification was conducted in reaction mixture using the TaqMan Universal PCR Master Mixture according to the protocol supplied by the manufacturer. Samples were analyzed with the ABI PRISM 7000 sequence detection system (Applied BioSystems). All PCRs were performed in triplicate, and the specificity of the reaction was determined by melting curve analysis at the dissociation stage. I synthesized specific primers for NFkB1 (forward 5'-CTGCTGACAATTTCCCACAC-3'; reverse 5'-GCTCTCTGAGC ACCTTTGGA-3'). The relative quantitative method was used for the quantitative analysis. The calibrator was the averaged ΔCt from the untreated cells and the endogenous controls were GAPDH for genes and U6B for miRNAs.

Western Blotting

Cells were harvested, and lysed, and proteins were separated on a SDS/polyacrylamide gel and transferred to a PVDF membrane (Bio-Rad, Hercules, CA, USA). After blocking, the membranes were incubated with the primary antibodies anti-ACTB and anti-NFkB1 polyclonal antibody (Santa Cruz Biotechnology, Santa Cruz, CA, USA). Membranes were extensively washed and incubated with a horseradish peroxidase-conjugated secondary antibody (Bio-Rad). The

antigen-antibody complexes were visualized by West-Q-Chemiluminescent Sub Kit Plus (BIOTANG, Waltham, MA, USA).

Luciferase assay

The 3' UTRs of NFkB1 were fused to the renilla gene using the XhoI/NotI restriction sites of the psiCHECK2vector (Promega). A total of 8*10^4 H1299 cells were co-transfected with 30 ng of the indicated vector and 90ng of the pcDNA3 cloned miR-26b using Fugene(HD) Roche for 48 hrs. Luciferase assays were performed using the Dual-Luciferase assay (Promega).Normalization of the Renilla expression was performed using the luciferase gene present on the psiCHECK2 vector.

MTT assay

H1299 cells were transfected with miR-9, miR26b, and let7g expression vector. Forty-eight hours after transfection, cells were seeded at 5,000/well into 96-well plates and exposed to various doses of IR at 0, 2, 4, and 6 Gy. After γ-irradiation, the cells were incubated for 5 days, MTT (3- (4, 5-dimethylthiazole)-2, 5-diphenyltetrazoliumbromide) assay reagents were added, and the absorbance was measured at 560 nm. All experiments were repeated at least three times, and data are presented as mean ± standard deviation (SD). The Student's t-test was used to compare the means of the different groups. A P-value of <0.05 was considered statistically significant.

RESULTS

Candidate Selection

In order to identify miRNAs that suppress NFkB1 expression, miRNA profiling is performed in H1299 lung cancer cells at 0, 2, 4, 8, 12, and 24 hours after 2 Gy γ-irradiation. miRNA list was filtered in a time series profile based on the target prediction using TargetScan (Lewis, Burge et al. 2005) and the correlation coefficient between NFkB1 and miRNAs. Among 328 human miRNAs in the microarray, I found that expression of miR-9, miR-424, and miR-195 was inversely correlated with expression of NFkB1 in γ-irradiated H1299 cells (Table 1). The expression patterns of these selected miRNAs are shown in a heatmap (Fig. 1). Among these selected miRNAs, I confirmed the expression of miR-9 and NFkB1 in γ-irradiated H1299 cells using real-time RT-PCR (Fig. 2). I used let-7g and miR-26b as controls, because these two miRNAs do not have binding sites in NFkB1 3'UTR. The expression of let-7g and miR-26b also decreased upon IR in H1299 cells, as did miR-9.

Table 1. List of miRNA profiles targeting NFkB1 in γ-irradiated H1299 cells

Genes	Expression of genes after g-irradiation Log2[Signal Intensity]						Pearson's correlation coefficient
	0 hr	2 hr	4 hr	8 hr	12 hr	24 hr	
NFkB1	8.95	9.01	9.31	9.43	9.36	9.00	
miR-424	6.32	6.00	6.29	4.23	4.98	5.44	-0.65
miR-9	5.80	5.95	5.90	4.29	4.46	4.40	-0.46
miR-195	7.84	7.38	8.32	6.87	7.09	7.20	-0.24
miR-183	4.05	4.11	3.41	5.57	5.40	5.35	0.33

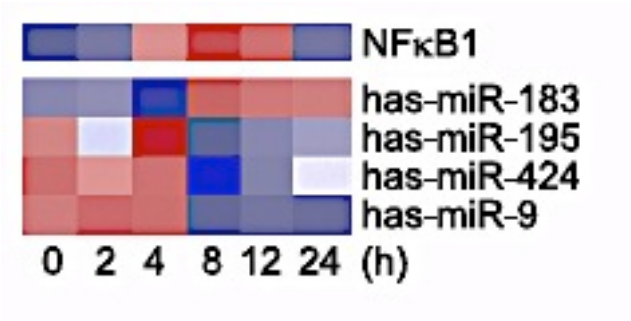

Fig 1. Heatmap analysis shows the expression of NFkB1 and miRNAs targeting NFkB1 in H1299 cells upon ionizing radiation at 0, 4, 8, and 12 hrs.

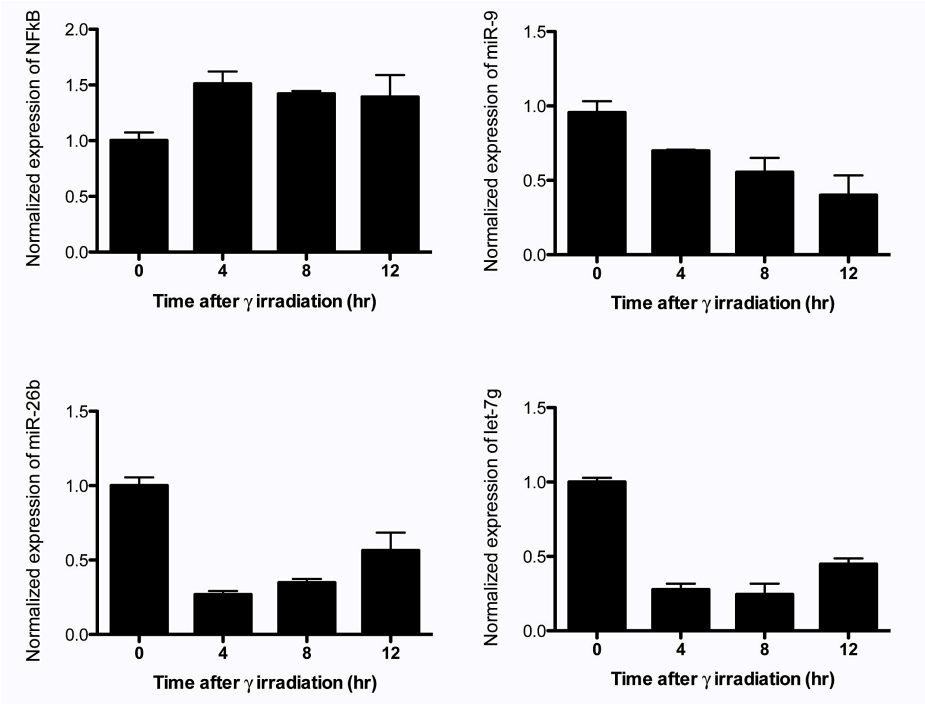

Fig 2. Expression patterns of NFkB1 and miRNAs in γ-irradiated H1299 cells. The expression of NFkB1 mRNA was quantitated with real-time RT-PCR at the indicated time. The values were normalized

with GAPDH mRNA. The expressions of miR-9, let-7g, and miR-26b were measured by real-time RT-PCR in γ-irradiated H1299 cells at the indicated time. U6B mRNA was used as a normalization control for miRNAs. All values are presented as mean ± SD from triplicate experiments.

miR-9 targets UTR of NFkB1

The miRNA miR-9 was previously found to be a candidate miRNA targeting NFkB1, (Bazzoni, Rossato et al. 2009), but its effect on radiosensitivity was not examined. There is one defined miR-9 target site at position 29-35 of NFkB1 3' UTR, as shown in Fig. 3A. I introduced a miR-9-expression vector into H1299 cells and then measured the expression of miR-9 using real-time RT-PCR. I used let-7g and miR-26b as controls to check the specific effect of miR-9 (Fig. 3B). miR-9 inhibited NFkB1 expression in real-time RT-PCR as well as in western blot analysis (Fig. 3C and 3D), indicating that a strong correlation between miR-9 and NFkB1 exists. To confirm that 3' UTR of NFkB1 has the binding site for miR-9 I cloned 3'UTR of the candidate gene downstream of the renilla luciferase reporter gene. MiR-9 target the NFkB1 gene was confirmed by the decrement in the Renilla activity (Fig. 3E). Interestingly, let-7g inhibited the expression of NFkB1 as much as miR-9, while miR-26b did not.

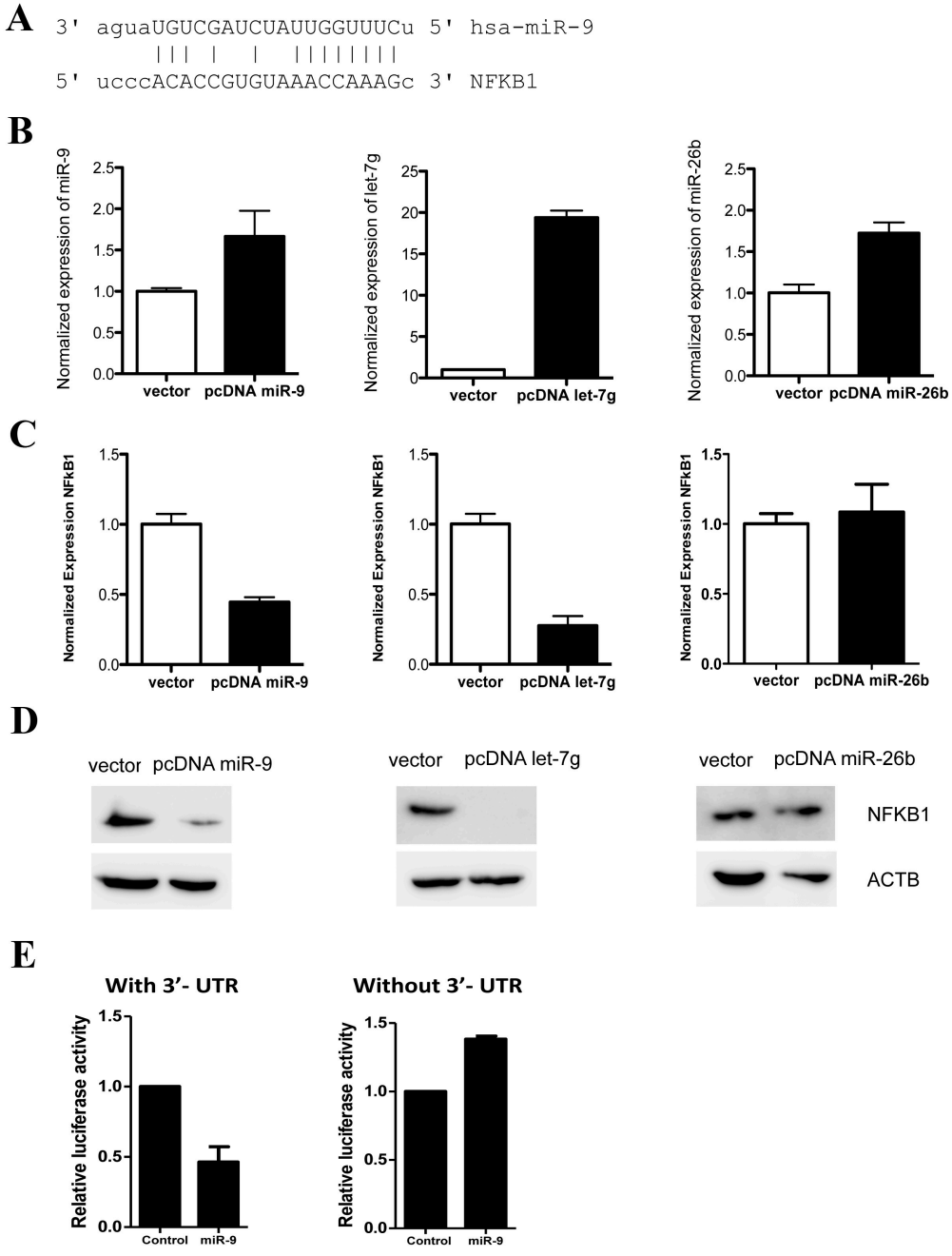
A
3' aguaUGUCGAUCUAUUGGUUUCu 5' hsa-miR-9
5' ucccACACCGUGUAAACCAAAGc 3' NFKB1
B
Normalized expression of miR-9
vector
pcDNA miR-9
Normalized expression of let-7g
vector
pcDNA let-7g
Normalized expression of miR-26b
vector
pcDNA miR-26b
C
Normalized Expression NFkB1
vector
pcDNA miR-9
Normalized Expression NFkB1
vector
pcDNA let-7g
Normalized Expression NFkB1
vector
pcDNA miR-26b
D
vector
pcDNA miR-9
vector
pcDNA let-7g
vector
pcDNA miR-26b
NFKB1
ACTB
E
With 3'- UTR
Relative luciferase activity
Control
miR-9
Without 3'- UTR
Relative luciferase activity
Control
miR-9

Fig 3. **Suppression of NFkB1 by miR-9 and let-7g.** (A) Target sequence of miR-9 in NFkB1 3'UTR was predicted by TargetScan. (B) In miR-9, let-7g, and miR-26b transfected H1299 cells, the expression of each miRNA was confirmed by real-time RT-PCR. (C) The expression of NFkB1 mRNA in miRNA-transfected cells was measured by real-time RT-PCR. The relative NFkB1 expression levels were normalized against GAPDH and presented as mean ± SD from triplicate experiments. (D) The protein levels of NFkB1 were also examined by western blot in miRNA-transfected cells. (E) Cells were transfected with the empty renilla luciferase reporter gene (psiCHECK2) or the reporter gene fused to the NFkB1 3' UTR. In addition, the cells were co-transfected with miR-9 or without miR-9. Results are expressed as relative light units (RLU) and were normalized with the luciferase activity expressed constitutively by the psiCHECK2 vector.

Role of miR-9 in sensitization

To study whether miR-9 could sensitize H1299 cells to IR, I first overexpressed miR-9 and measured cell survival upon γ-irradiation at 0, 2, 4, and 6 Gy using the MTT assay (Fig. 4). I used let-7g and miR-26b as controls, since there are no binding sites for these miRNAs in NFkB1 3'UTR sequences. miR-9 suppressed the expression of NFkB1 at both the mRNA and protein level (Fig. 3D), and significantly sensitized H1299 cells to IR in a survival analysis. Interestingly, let-7g also suppressed the expression of NFkB1 as much as miR-9 did, and also enhanced the sensitivity of H1299 cells to γ-irradiation. The expression of miR-26b did not alter the expression of NFkB1 or cell survival. In order to testify the miRNA mediated sensitization in other cell lines I selected A549 cells and performed the MTT assay by first overexpressing miR-9 and then measuring the cell survival upon γ-irradiation at 0, 2, 4, and 6 Gy respectively (Fig. 5B)

I also measured the expression patterns of NFkB1 in miR-9 and let-7g transfected cells upon IR (Fig. 5A). The increase in NFkB1 expression is inhibited in miR-9 and let-7g transfected cells, suggesting that the expression of NFkB1 in γ-irradiated cells was regulated by the down-regulation of miR-9 and let-7g. These results demonstrate that miR-9 and let-7g suppress the expression of NFkB1 and enhance the sensitivity to IR in H1299 lung cancer cells (Fig. 5C).

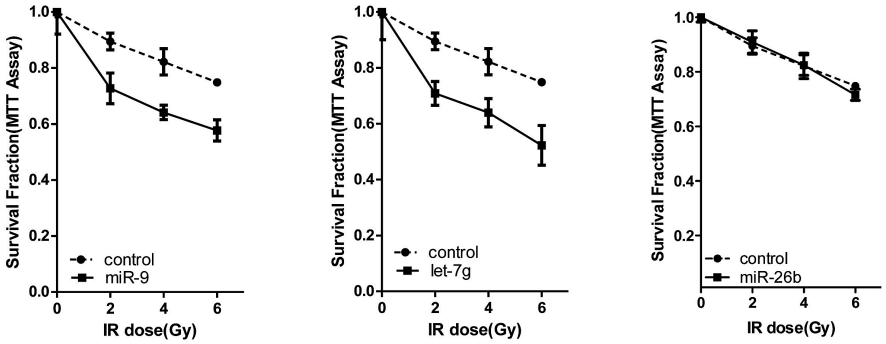

Fig 4. **miR-9 and let-7g enhance the sensitivity to ionizing radiation in H1299 cells**. miR-9, let7g, and miR-26b were overexpressed and the cell survival fraction upon γ-irradiation was measured using MTT assay in H1299 cells.

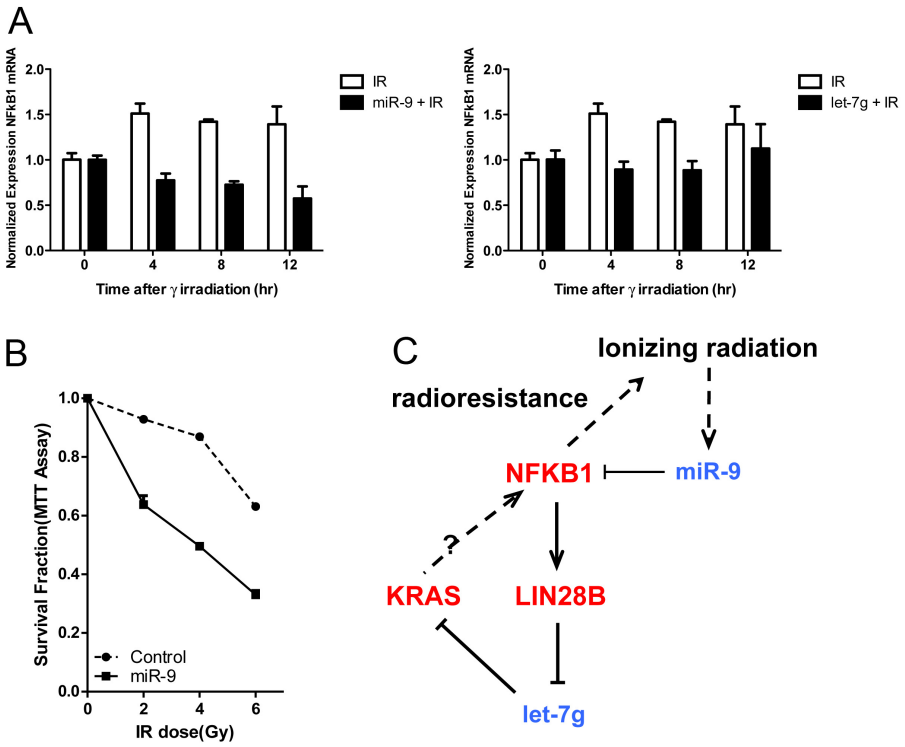

Fig. 5 Impact of miR-9 on IR induced changes. (A) The expression of NFkB1 was measured in miRNA-transfected cells after γ-irradiation. (B) miR-9 was overexpressed and the cell survival fraction upon γ-irradiation was measured using MTT assay in A549 cells. (C) miR-9 can directly control the expression of NFkB1, and the indirect regulation of NFkB1 by let-7g may be proposed to control radiosensitivity.

DISCUSSION

In γ-irradiated H1299 human lung cancer cells, expression of miR-9 was down regulated while the expression of NFkB1 was up regulated. Both miR-9 and let-7g suppressed the expression of NFkB1, which resulted in increased sensitivity to IR in the H1299 human lung cancer cell line. Given these results, I suggest that miR-9 and let-7g may play an important role in the response to ionizing radiation through the inhibition of NFkB1. IR can induce DNA damage by inducing progressive changes in cell survival, growth, and proliferation by affecting gene expression (Amundson, Bittner et al. 2003). Previous reports suggest that radiation can change the expression pattern of some genes (Park, Hwang et al. 2002; Smirnov, Morley et al. 2009). NFkB1 has been previously suggested to alter the sensitivity to radiation and chemotherapeutic agents (Janssens and Tschopp 2006; Perkins and Gilmore 2006). Here I show that NFkB1 is targeted by miR-9 and let-7g, which results in the increased sensitivity to IR.

The let-7 family of miRNAs regulates expression of oncogenes, such as RAS, and is specifically down regulated in many cancer subtypes. Low levels of let-7 predict a poor outcome in lung cancer. The let-7 family of miRNAs is overrepresented in a class of miRNAs exhibiting altered expression in response to radiation. The let-7 family of miRNAs can suppress resistance to anticancer cytotoxic therapy, including radiotherapy. In the present study, let-7g sensitized the H1299 cells but also suppressed the expression of NFkB1. Recently, Iliopoulos et al. (2009) reported that let-7g can suppress the expression of RAS, and

ultimately suppress the expression of NFkB1. In a previous report, it was shown that increased let-7g suppressed KRAS in H1299 cells (Jeong, Wu et al. 2009). This study examined miRNAs in radioresistance lung cancer cell lines and concludes that miR-9 and let-7g can regulate the sensitization of cells by interacting with NFkB1. Along with NFkB1 there are other member genes like Lin28B, KRAS etc. which might be playing a crucial role in the overall regulation by interacting with each other and with miRNAs (Fig. 5C). It is likely that miRNAs act in a similar dominant manner in radiation-induced DNA damage responses in other cancer types as well.

REFERENCES

Aggarwal, B. B., R. V. Vijayalekshmi, et al. (2009). "Targeting inflammatory pathways for prevention and therapy of cancer: short-term friend, long-term foe." Clin Cancer Res **15**(2): 425-430.

Amundson, S. A. (2008). "Functional genomics in radiation biology: a gateway to cellular systems-level studies." Radiat Environ Biophys **47**(1): 25-31.

Amundson, S. A., M. Bittner, et al. (2003). "Functional genomics as a window on radiation stress signaling." Oncogene **22**(37): 5828-5833.

Bazzoni, F., M. Rossato, et al. (2009). "Induction and regulatory function of miR-9 in human monocytes and neutrophils exposed to proinflammatory signals." Proc Natl Acad Sci U S A **106**(13): 5282-5287.

Chaudhry, M. A., B. Kreger, et al. (2010). "Transcriptional modulation of micro-RNA in human cells differing in radiation sensitivity." Int J Radiat Biol **86**(7): 569-583.

Chen, X. P., L. Y. Tao, et al. (2002). "[Influence of NF-kappa B on the development and regulation of neural system]." Fa Yi Xue Za Zhi **18**(2): 112-114.

Huber, W., A. von Heydebreck, et al. (2002). "Variance stabilization applied to microarray data calibration and to the quantification of differential expression." Bioinformatics **18 Suppl 1**: S96-104.

Janssens, S., A. Tinel, et al. (2005). "PIDD mediates NF-kappaB activation in response to DNA damage." Cell **123**(6): 1079-1092.

Janssens, S. and J. Tschopp (2006). "Signals from within: the DNA-damage-induced NF-kappaB response." Cell Death Differ **13**(5): 773-784.

Jeong, S. H., H. G. Wu, et al. (2009). "LIN28B confers radio-resistance through the posttranscriptional control of KRAS." Exp Mol Med **41**(12): 912-918.

Kunnumakkara, A. B., P. Diagaradjane, et al. (2008). "Curcumin sensitizes human colorectal cancer xenografts in nude mice to gamma-radiation by targeting nuclear factor-kappaB-regulated gene products." Clin Cancer Res **14**(7): 2128-2136.

Kwak, H., K. C. Jeong, et al. (2009). "Flavonoids inhibit the AU-rich element binding of HuC." BMB Rep **42**(1): 41-46.

Lewis, B. P., C. B. Burge, et al. (2005). "Conserved seed pairing, often flanked by adenosines, indicates that thousands of human genes are miRNA targets." Cell **120**(1): 15-20.

Li, F. and G. Sethi (2010). "Targeting transcription factor NF-kappaB to overcome chemoresistance and radioresistance in cancer therapy." Biochim Biophys Acta **1805**(2): 167-180.

Park, W. Y., C. I. Hwang, et al. (2002). "Identification of radiation-specific responses from gene expression profile." Oncogene **21**(55): 8521-8528.

Perkins, N. D. and T. D. Gilmore (2006). "Good cop, bad cop: the different faces of NF-kappaB." Cell Death Differ **13**(5): 759-772.

Preston, R. J. (2005). "Radiation biology: concepts for radiation protection." Health Phys **88**(6): 545-556.

Smirnov, D. A., M. Morley, et al. (2009). "Genetic analysis of radiation-induced changes in human gene expression." Nature **459**(7246): 587-591.

Sung, H. Y., H. G. Wu, et al. (2010). "Dcr3 inhibit p53-dependent apoptosis in gamma-irradiated lung cancer cells." Int J Radiat Biol **86**(9): 780-790.

Voboril, R. and J. Weberova-Voborilova (2007). "Sensitization of colorectal cancer cells to irradiation by IL-4 and IL-10 is associated with inhibition of NF-kappaB." Neoplasma **54**(6): 495-502.

Weidhaas, J. B., I. Babar, et al. (2007). "MiRNAs as potential agents to alter resistance to cytotoxic anticancer therapy." Cancer Res **67**(23): 11111-11116.

Chapter II

Role of PRDM5 in radio- and chemo-sensitization of NSCLC's

ABSTRACT

Non-small cell lung cancer (NSCLC) is a remarkably heterogeneous disease and remains largely incurable due to resistance developed against the drugs and ionizing radiations. In the present study I have shown the role of PRDM5 gene, whose precise function remained elucidated till now. I found that it is highly expressed in the NSCLC. Knockdown of the PRDM5 reduced the growth of cancer cell as well as it leads to the radio and chemo sensitization of NSCLCs.

I the present study I proposed a mechanism in which PRDM5 binds to the promoter of miR-135b, thereby leading to its suppression. This abrogation leads to high expression of HIF1α, which is a target of miR-135b.

To detect the expression of PRDM5 in NSCLC's I performed QRT-PCR and western blotting and found that it is highly expressed in cell line, also I found in GEO data sets that PRDM5 is highly expressed in lung cancer patients. Next I analyzed the role of PRDM5 in the relapse free survival considering the various GEO datasets and found that ADC and SCC patients who have high expression of PRDM5 have lower rate of relapse free survival. In order to show the association between PRDM5 and miR-135b I performed CHIP (chromatin immune-precipitation) assay. Correlation between PRDM5, miR-135b, HIF1α and VEGF is shown via RT-PCR and western blotting (VEGF is considered as a marker of HIF1α in the present study). I have demonstrated that PRDM5 binds to the miR-135b . Inhibition of

PRDM5 leads to the up regulation of miR-135b, which leads to the suppression of HIF1α (direct target) leading to the growth inhibition, radiosensitization and chemo sensitization.
(MTT assay and clonogenic assays were performed to show the role of PRDM5 and miR-135b in dual sensitization).
Together I provided a new insight into the multiple effects of PRDM5 in NSCLC. I discovered that PRDM5, when inhibited reduced the cell growth as leads to the dual sensitization, suggesting that PRDM5 is a high quality target in NSCLC. A strong correlation between PRDM5 and HIF1α is demonstrated at both cell line as well as patient level. In addition to this, I also found that miR-135b acts as a tumor suppressor miRNA for NSCLC which inhibits the growth and progression of NSCLC as well as leads to radio and chemo sensitization.

Keywords: NSCLC, PRDM5, HIF1α and miR-135b, Radio and chemo sensitization.

INTRODUCTION

Every year approximately 7.3 million people die because of cancer and lung cancer is the cause of about 1.3 million deaths. Lung cancer is basically divided into two types: small cell lung cancer(SCLC) and non-small cell lung cancer(NSCLC). Approximately 85% of total lung cancers are NSCLC which are further classified into two subtypes : squamous cell carcinoma(SCC) and adenocarcinoma(AD). Several markers of lung cancer have been studied such as KRAS, HER2, LKB1, BRAF etc which helped in understanding the metastatic potential and growth of tumor cells in order to perform targeted therapy.

MiRNAs are short 20–25 nucleotide RNA molecules that are transcribed by RNA polymerase II and negatively regulate gene expression by targeting the 3'UTRs of mRNAs(Bartel 2004; Bartel 2009). miRNA expression can be regulated by transcription factor (TF)binding sites present in their promoters (Xi, Shalgi et al. 2006; Zhou, Ferguson et al. 2007; Chang, Yu et al. 2008; Schanen and Li 2011). At the post-transcriptional level, miRNAs are involved in many biological processes, including development (Marson, Levine et al. 2008), proliferation, cell death (Brennecke, Hipfner et al. 2003), epithelial-mesenchymal transition(Chang, Chao et al. 2011) and tumorigenesis (Kent and Mendell 2006) by interacting with the genes which are crucial players of these processes like p53 (Chang, Chao et al. 2011), NFKB1 (Arora, Qureshi et al. 2011), HIF1 (Yamakuchi,

Lotterman et al. 2010), FMR1or FXR1(Gessert, Bugner et al. 2010) etc. Many studies have analyzed the transcriptional regulation of mRNAs and miRNAs in radiation exposed or drug treated cells to understand cellular responses to ionizing radiation (IR) or drugs (Weidhaas, Babar et al. 2007; Jeong, Wu et al. 2009; Chen, Zuo et al. 2010; Arora, Qureshi et al. 2011; Zhang, Yang et al. 2011).

Normally when the cancer cells are exposed to radiations or drugs there occurs certain changes in the expression of genes and miRNAs as reported by certain studies (Shin, Cha et al. 2009; Simone, Soule et al. 2009; Oliveras-Ferraros, Cufi et al. 2011). It is supposed that, out of these changes there could be some that could be the reason for the induction of resistance in the cancer cells towards the radiations and drugs. Among the various genes, which are known for the resistance, one of the well known is hypoxia-inducible factor 1 alpha (HIF1α) (Semenza 2004; Harada, Itasaka et al. 2009), it is the transcription factor that mediates the metabolic switch from oxidative phosphorylation to aerobic glycolysis in response to hypoxia, it is known to be induced by ionizing radiations and regulate the expression of VEGF and bFGF in tumor cells, which promotes the cancer cell survival(Semenza 2004), there are some studies, which indicated that NFkB plays a role in the regulation of HIF1α induction (Belaiba, Bonello et al. 2007; Nam, Ko et al. 2011). However the exact molecular mechanism behind the regulation of induction of resistance towards drugs and radiations via HIF1α is unclear till now. In the present study I studied the molecular mechanism behind the resistance development

that involves HIF1α, in resistant human lung cancer cells A549 [p53 positive] and H1299 [p53 null].

The human PRDM gene family consists of 17 known members characterized by the presence, generally at the N-terminus, of the PR domain, related to the SET domain functioning in chromatin-mediated transcriptional regulation (Schneider, Bannister et al. 2002), followed by a variable number of zinc finger repeats. PRDM5 (or PFM2) is a recently characterized member of the PRDM family. Upon PRDM5 over-expression, different genes encoding proteins involved in cell adhesion (CNTN3, CNTNAP2, NINJ1) (Araki and Milbrandt 1996; Poliak, Gollan et al. 1999), components of extracellular matrix (COL5A1, COL6A3, FBLN1, MFAP5) (Gibson, Leavesley et al. 1999; Timpl, Sasaki et al. 2003) or proteins involved in regulation of extra cellular matrix (ECM) production (FOXF2) (Ormestad, Astorga et al. 2006) are down regulated, suggesting that PRDM5 negatively modulates cell-cell and cell-matrix adhesion. Although its precise biological function remains to be elucidated, inactivation of PRDM5 in different tumors suggests that it may behave as a tumor suppressor. It is, in fact, often silenced in cell lines derived from breast, ovarian and hepatic tumors (Deng and Huang 2004) and has been identified as a target of epigenetic silencing in colorectal and gastric cancer (Watanabe, Toyota et al. 2007). PRDM5 has been shown recently to negatively modulate both the canonical wnt/b-catenin pathway and the non-canonical planar cell polarity (PCP) wnt pathway (Meani, Pezzimenti et al. 2009).

In this study I found that upon radiation or drug exposure the expression of PRDM5 is induced in lung cancer cells. PRDM5 binds with the promoter of several miRNAs, after closure analysis I selected miR-135b from the list of different miRNA which could be regulated by PRDM5 binding. miR-135b is predicted to target the 3'UTR of HIF1α. I studied the regulation of PRDM5, miR-135b and HIF1α upon ionizing radiations and drug treatment.

MATERIALS AND METHODS

Cell Culture

H1299, A549, H460, H1573, H23, HCC1438, H1975 and H226 cells were maintained in RPMI 1640 medium supplemented with 10% fetal bovine serum, 100units/ml penicillin, 100 mg/ml streptomycin and 2mM-L glutamine. Normal human SAECs and specific medium were purchased from Promo cell (Heidelberg, Germany). SAECs were maintained in serum-free SAGM supplemented with bovine pituitary extract, 10 ng/ml epidermal growth factor,.5ug/ml hydrocortisone,.5ug/ml epinephrine,10ug/ml transferrin and .1ng/ml retinoic acid. The cultured cells were either exposed to 0-10 Gy of radiation using a 4-MV linear accelerator (Clinac 4/100 ,Varian, Palo Alto ,CA) or left irradiated as a negative control.

Plasmids

The precursor of miR-135b was amplified from the A549 genomic DNA, was first cloned into PGEMT easy vector (Promega ,Madison,WI) and than sub cloned into pcDNA3 Vector. PRDM5 CDS region was amplified using cDNA of A549 cells, directly cloned into pcDNA3 (Invitrogen). Total RNA for real-time PCR, protein for western blot, and cell for MTT assay were collected after 48h of transfection (Table 3).

RNA preparation and quantitative real-time PCR

Total RNA was extracted from cell lines using the TRIzol method, and then reverse transcribed to complementary DNA using Superscript II reverse transcriptase (Invitrogen, Carlsbad, CA, USA) and oligo-(dT)12–18 primers according to the manufacturer's protocol. The quantitative RT-PCR for indicated genes was performed in a reaction mixture containing SYBR Premix Ex Taq (Takara Bio Inc., Shiga, Japan). Quantitation of miRNAs was performed using TaqMan miRNA assays (Applied Biosystems, Foster City, CA, USA) according to the manufacturer's protocol. Samples were analyzed using the ABI PRISM 7000 sequence detection system (Applied BioSystems). All PCRs were performed in triplicate, and the specificity of the reaction was determined by melting curve analysis at the dissociation stage. I synthesized specific primers for PRDM5 ,HIF1A and VEGF . The relative quantitative method was used for the quantitative analysis. The calibrator was the averaged ΔCt from the untreated cells. The endogenous control was glyceraldehyde 3-phosphate dehydrogenase (GAPDH) for genes and U6B for miRNAs (Table 3).

Luciferase assay

The 3' UTRs of HIF1α were fused to the renilla gene using the XhoI/NotI restriction sites of the psiCHECK2vector (Promega). Primer used to amplify 3'UTR are listed in Table 3. A total of 8*10^4 A549 cells were co-transfected with 30 ng of the indicated vector and 90ng of the pcDNA3 cloned miR-135b using Fugene(HD) Roche for 48 hrs. Luciferase assays were performed using the Dual-Luciferase assay (Promega). Normalization of the Renilla expression was performed

using the luciferase gene present on the psiCHECK2 vector. For the promoter activity cell were transfected with reporter plasmid, and the TK-Renilla reporter (Promega) was also co-transfected for normalization of transfection efficiency. Transfected cells were treated with doxorubicin and harvested at 48hrs post-transfection, and a dual luciferase assay was performed according to the manufacturer's instruction (Promega) All experiment were performed in triplicates and repeated at least twice.

Western blotting

Cells were harvested and lysed in NP-40 buffer containing phenyl methyl sulfonyl fluoride and Protease Inhibitor Cocktail (Sigma, St. Louis, MO, USA). Protein extracts were then separated by sodium dodecyl sulfate-polyacrylamide gel electrophoresis, and then transferred to poly-vinylidene fluoride membranes (Bio-Rad, Hercules, CA, USA). Membranes were incubated with PRDM5(Abfrontier),HIF1A(BD Biosciences) and VEGF antibodies (1:1000; Santa Cruz Biotechnology Inc.) in Tris-buffered saline Tween 20 buffer with non-fat dry milk, and then incubated with horseradish peroxidase-conjugated secondary antibodies (dilution 1:5000; Bio-Rad). Immunoreactive bands were visualized using the Thermo Scientific Chemi-luminiscent Pico Kit.

MTT assay

H1299, A549, H1573 cells were transfected with miR 135b and siPRDM5 (Bioneer). Forty eight hours after transfection, cells were

seeded into 96-wells plates in triplicate and were either exposed to various doses of IR at 0,2,4 and 6 Gy, followed by incubation of 5 days or treated with 2.5nM, 5nM and 10nM of doxorubicin followed by incubation of 48hrs.MTT (3-(4,5-dimethylthiazole)-2,5-diphenyltetrazoliumbromide)assay reagents were added and the absorbance was measured at 560nm.For clonogenic assay the transfected cells were plated and were exposed to 10nM of doxorubicin drug ,the cell were cultured for approximately two weeks ,depending on the cell line. The colonies were fixed and stained with crystal violet.

ChIP assay

Chromatin immunoprecipitation experiment was performed considering EZ-CHIP (Upstate) protocol using PRDM5 antibody (Santa Cruz).

Statistical analysis

Results were reported as mean ± s.e.m. (s.e.m.). Independent Student's t test or the Wilcoxon signed-rank test was performed to analyze gene and miRNA expression levels and data. The log-rank test was used to test for differences in survival in univariate analysis. Expression values were introduced into survival analysis as continuous variables using a nonparametric approach in which samples were ranked by expression values and ranks were normalized between 0 and 1. Statistical analyses were performed using R. DRFS and RFS were calculated as described by the STEEP criteria33.

miR-135b and HIF1α expression levels across NCI-60

The normalized mRNA and miRNA expression data were obtained from GEO using series matrix files of datasets GSE32474 (mRNA) and GSE26375 (miRNA). Correlation between groups was assessed by Spearman correlation [r], with $P < 0.05$ being considered significant.

RESULTS

PRDM5 Expression in Lung Cancer Cells

In the first step, I checked the basal expression of PRDM5 in different NSCLC lung cell lines; I found that the expression of PRDM5 is induced in all the cell lines as compared to that of control normal cell both at mRNA and at protein level (Fig. 1A and 1B).

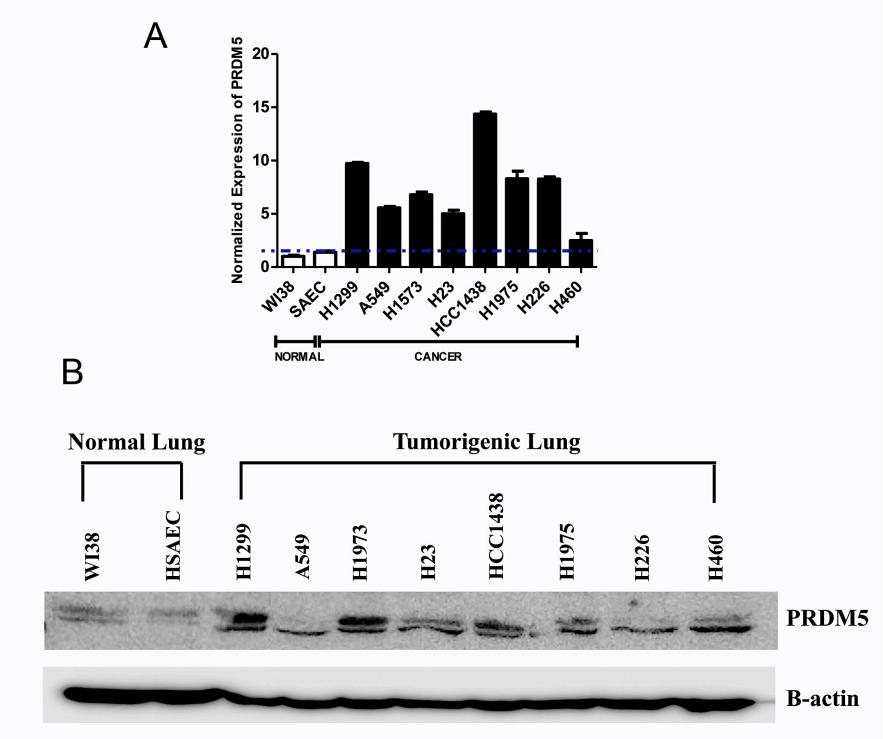

Fig. 1 PRDM5 expression in lung cancer cell lines. A) Quantative RT-PCR analysis and B) western blot showed that relative PRDM5 expression levels is high in human NSCLC cancer cell lines (H1299, A549, H1573, H23, HCC1438, H1975, H226 and H460) when compared normal lung cancer cell lines (WI38 and HSAEC).

PRDM5 expression is found to be high in NSCLC Lung Cancer Patients

Enrichment analysis is done considering the GEO datasets [GSE10799, GSE12667, GSE19188, & GSE10245 respectively]. There were three probe sets of PRDM5, out of which I considered two (ID-1569608_at and 220792_at respectively) considering the fact that the sensitivity of these two probe sets is higher than 0.5. After combining the patients from all the 4 GEO datasets, I finally got 221 patients data. Interestingly I found that the expression of PRDM5 (averaging the expression of PRDM5 in two probe sets) in lung cancer tissues is induced in more than 53.8% patients (Fig. 2A and 2B).

Also, considering the GEO data GSE7670, I found that the expression of PRDM5 is significantly LOW in 59.25 % of adjacent normal tissues as compared to that of tumor tissues the same lung cancer patients (Fig. 2C).

Clinical significance of PRDM5

In order to understand the clinical significance of PRDM5, I performed a retrospective analysis on a series of lung cancer samples considering and combining PRDM5 gene expression in patients from GEO datasets GSE3141 (SCC) and GSE5843 (ADC) respectively (n=99). The samples were divided into two sets (high and low expression of PRDM5) on the basis of median score ($P < 0.05$). PRDM5 showed a significant association with relapse free survival (Fig. 3; $P < 0.05$) (Table 1).

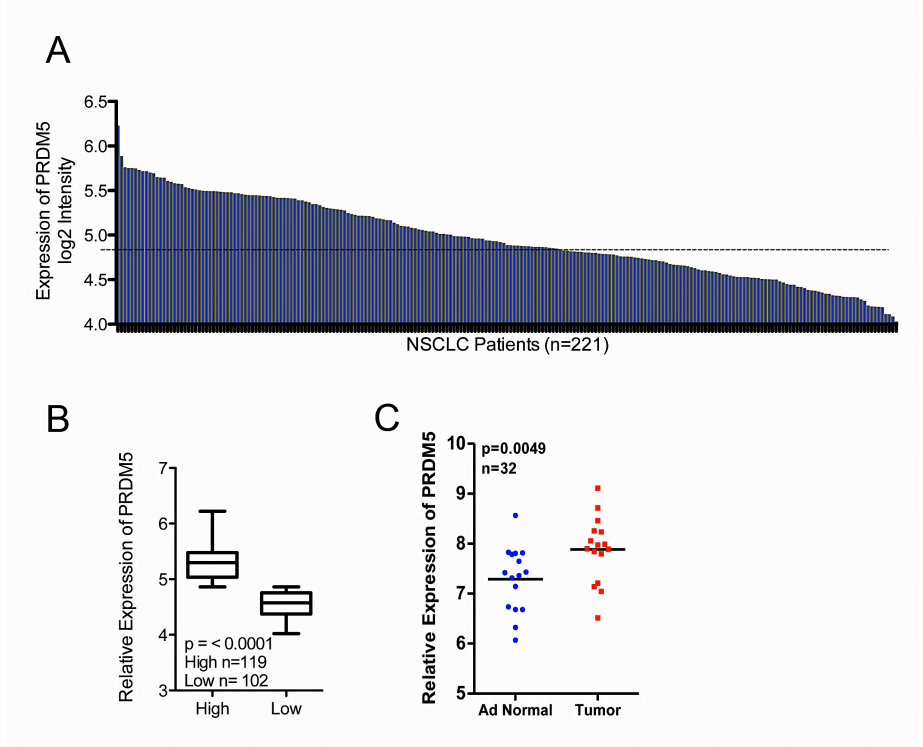

Fig. 2 PRDM5 expression analysis in patients. A) and B) PRDM5 expression is found to be high in NSCLC lung cancer patient tissue (n=221) when compared with the normal lung cancer tissue (n=72)(represented by black dotted line). C) Expression of PRDM5 is found to be low in adjacent normal than that of the tumor tissues from the same lung cancer patients.

.

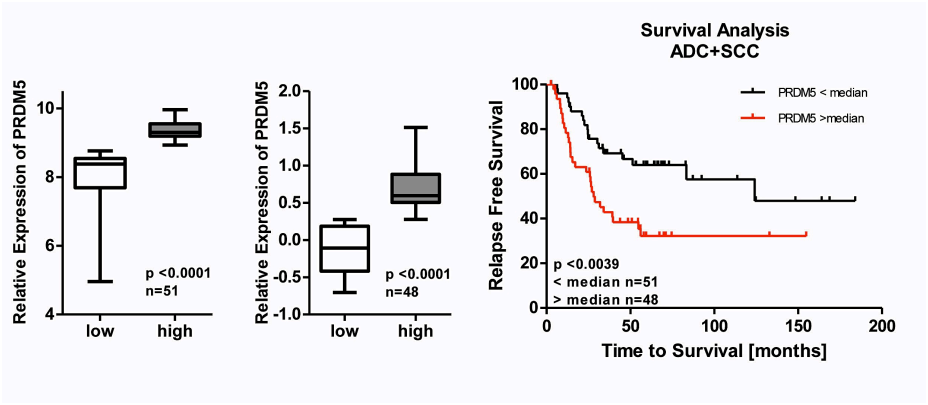

Fig. 3 Clinical significance of PRDM5. Relative expression of PRDM5 is found to be high in patient having SCC lung cancer (n=51; p=<.0001) and in patient having ADC lung cancer (n=48; P=<.0001). Kaplan Meier curves showing the RFS of subjects with high or low PRDM5 expression (n=99;p=0.0039). Log rank test was performed for checking the significant impact in the Kaplan Meier curves.

Inhibition of PRDM5 reduce the number of colony in the three cell lines

A colony-forming assay was carried out to evaluate the effect of PRDM5 inhibition on the clonogenic ability of lung cancer cells. siPRDM5 transfected A549, H1299 & H1573 cells displayed fewer colonies compared with that of the control (Fig. 4) .

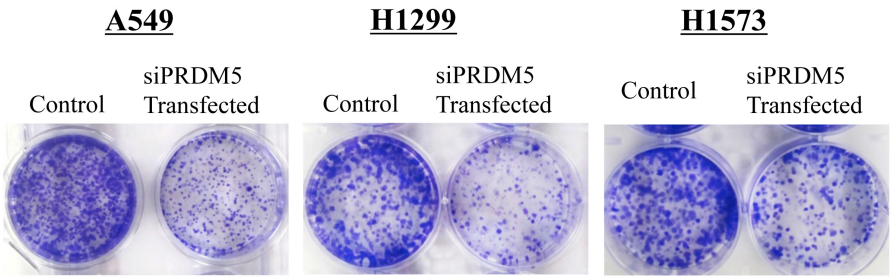

Fig. 4 Impact of PRDM5 inhibition on colony formation ability of lung cancer cells. Clonogenic assays shows that cell transfected with siPRDM5 have low colony number when compared with the control in 3 cell lines (A549, H1299 and H1573).

PRDM5 interact with miR-135b promoter

I referred to the findings by Marshall S. Horwitz and selected the miRNAs [miR-135b, miR-337, miR-143, miR-220, miR-5p, miR-145, miR-50 & miR-21] to which PRDM5 is reported to bind (Duan, Person et al.). As I wanted to study the role of PRDM5 in lung cancer and in the development of resistance towards DNA damaging agents, I considered HIF1α as my study candidate because it is commonly expressed in NSCLC and is associated with a number of biologic factors that are involved in the pathogenesis of lung cancer (Hatziapostolou and Iliopoulos 2011). With the help of various prediction tools I find out that miR-135b targets HIF1α.

I confirmed by chromatin immuno-precipitation assay that there is a interaction between PRDM5 and the promoter region of miR-135b by using the primers provided by Duan, Person et al. (Fig.5a). By qRT-PCR, I found a negative correlation between PRDM5 and miR-135b in different NSCLC cell lines (Fig. 5b).

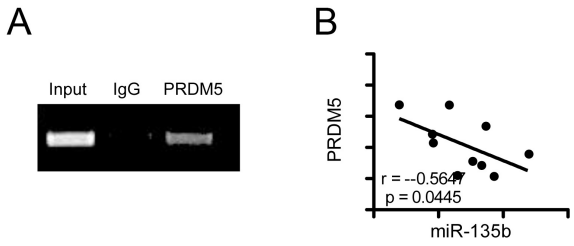

Fig. 5 PRDM5 binds upstream of promoter of miR-135b.

A) Binding of PRDM5 to the promoter region of miR-135b was shown by CHIP assays. Input 5% of total chromatin. B) Correlation plot extracted from different NSCLC cell lines showing that PRDM5 and miR135b is inversely correlated (R=-0.5647,P=0.0445) by Pearson's test.

MiR-135b Targets the 3'UTR of HIF1α

With the help of prediction tool I found that miR-135b target HIF1α. Next, to show the interaction between HIF1α and miR-135b, I overexpressed in miR-135b in A549 and H1299 cells respectively, and then performed real time PCR and results confirmed the miR-135b induced down regulation of HIF1α at RNA (Fig 6A and 6B). To prove that miR-135b can directly target the 3'UTR of HIF1α, I cloned the 3'UTR untranslated region (3'UTR) segment of HIF1α containing the predicted miR-135b target site into psicheck-2 vector, and empty vector is used as control. Each of the reporter constructs was co-transfected with miR-135b into A549 cells. Luciferase reporter assay confirmed that miR-135b reduced the activity of the reporter with a wild type 3'UTR (Fig 6C).

The HIF1α mRNA level was significantly inversely correlated with miR-135b expression when evaluated using the US National Cancer Institute's NCI60 database, which contains a panel of 60 diverse human cancer cell lines (Fig 6D).Also I found negative correlation between mRNA of HIF1α and miRNA135b in different NSCLC cell line (Fig 6E) (Table 2). It is well known that VEGF is downstream of HIF1α, so I checked the impact of miR-135b on the suppression of VEGF. QRT and Western blot results confirmed that over-expression of miR-135b down regulates VEGF (Fig 6F). From this I concluded that miR-135b down regulate the HIF1α protein which further down regulate VEGF mRNA and protein. Also I found a negative correlation between miRNA135b and VEGF mRNA(R=-0.549 ;P=.06).(Fig 6F).

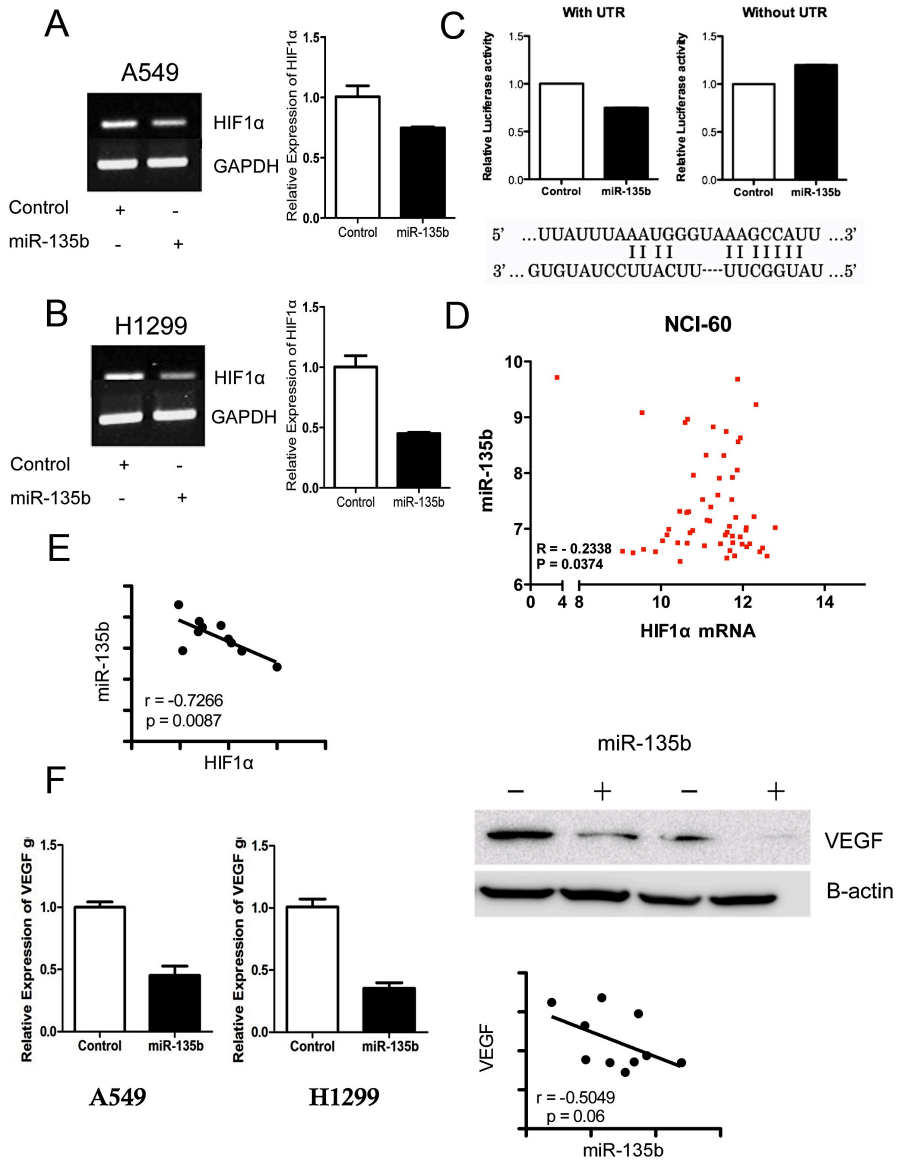
A
A549
HIF1α
GAPDH
Control + -
miR-135b - +
Relative Expression of HIF1α
Control
miR-135b
B
H1299
HIF1α
GAPDH
Control + -
miR-135b - +
Relative Expression of HIF1α
Control
miR-135b
C
With UTR
Without UTR
Relative Luciferase activity
Control
miR-135b
5' ...UUAUUUAAAUGGGUAAAGCCAUU ...3'
3' ... GUGUAUCCUUACUU----UUCGGUAU ...5'
D
NCI-60
miR-135b
HIF1α mRNA
R = - 0.2338
P = 0.0374
E
miR-135b
HIF1α
r = -0.7266
p = 0.0087
F
Relative Expression of VEGF
Control
miR-135b
A549
H1299
miR-135b
VEGF
B-actin
VEGF
miR-135b
r = -0.5049
p = 0.06

Fig. 6 miR-135 targets HIF1α. RT and QRT PCR shows down regulation of HIF1α mRNA when miR-135b is overexpressed when compared with the control in two cell line A) A549 and B) H1299. C) Luciferase reporter assay to examine the interaction between miR135b and the predicted site in the HIF1α in 3'UTR.Plasmid with the 3'UTRs or no UTR were co-transfected with the miR-135b. Renilla luciferase activity was measured by a Dual –luciferase Reporter Assay System and normalized to internal control firefly luciferase activity**.** D) Correlation plot extracted from NCI60 microarray data sets showing the HIF1α and miR-135b is inversely correlated with endogenous miR-135b(R=-0.2383;P=.0374 by Pearson's test **.** E) Inverse correlation found between HIF1α and miR-135b in different cell line (R=-0.7266; P=0.0087). F) QRT and western blot shows that overexpression of miR-135b leads to the down regulation of VEGF. Inverse correlation found between VEGF and miR-135b in different cell line (R=-0.5049; P=0.06).

miR-135b over-expression reduces the colony number of NSCLC'S

A colony-forming assay was carried out to evaluate the effect of miR-135b over expression on the clonogenic ability of lung cancer cells. miR-135b transfected A549 , H1299 and H1573 cells displayed fewer number of colonies compared with that of control (Fig. 7A).

Clinical significance of miR-135b

In order to understand the clinical significance of miR-135b, I considered the GEO data GSE16025 that comprised of 10 normal lung tissue samples and 61 tumor tissue samples. I found that the expression of miR-135b was significantly high in normal tissues as compared to tumor tissues (Fig. 7B). Apart from this, I considered GEO dataset GSE15008 which comprised of 116 pairs of primary lung cancers with their corresponding adjacent normal lung tissues collected a minimum of 5 cm from the tumor, and I found that the expression of PRDM5 is significantly High in 37.8% of adjacent normal tissues as compared to that of tumor tissues the same lung cancer patients (Fig. 7C).

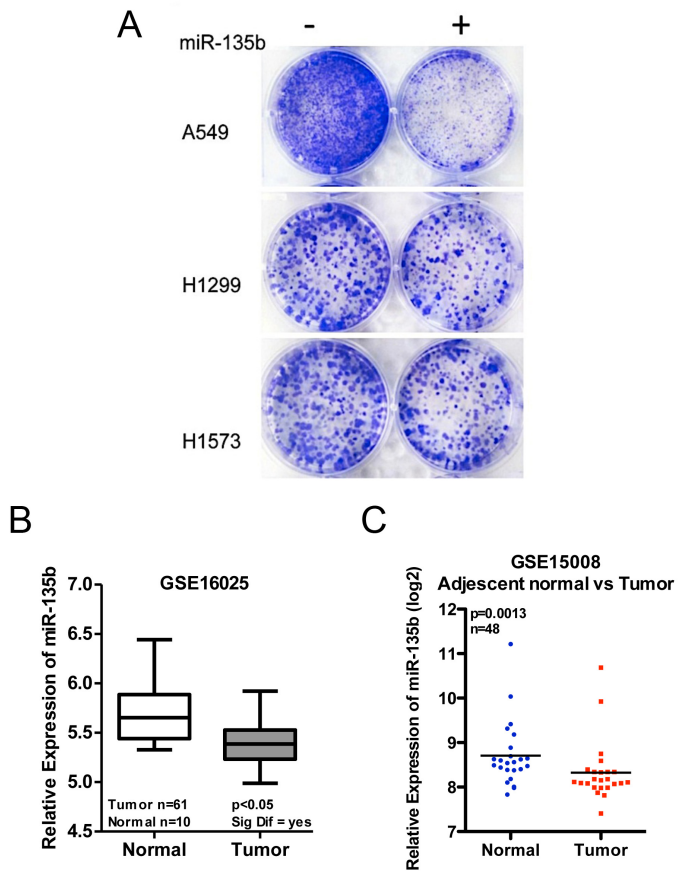

Fig. 7 miR-135b is suppressed in lung cancer patients and its over-expression suppresses colony formation ability of cancer cells.

A) Clonogenic assay showing miR-135b overexpression leads to the inhibition of colony formation in (H1299, A549 and H1573) cell line. B) Expression of miR-135b in normal vs lung tumor tissues. C) Relative expression of miR-135b in normal adjacent vs tumor tissues from same lung cancer patients.

Interaction between PRDM5, miR-135b, and HIF1α upon PRDM5 inhibition

In order to study the interaction between PRDM5, miR-135b, and HIF1α, I suppressed the PRDM5 gene with the siRNA transfection and checked the expression of other candidates. I found that PRDM5 suppression leads to the induction of miR-135b and reduction of the expression of HIF1α and VEGF respectively at RNA in both A549 (Fig 8A) and H1299 (Fig 8B) cells (VEGF is used as a marker for HIF1α expression).

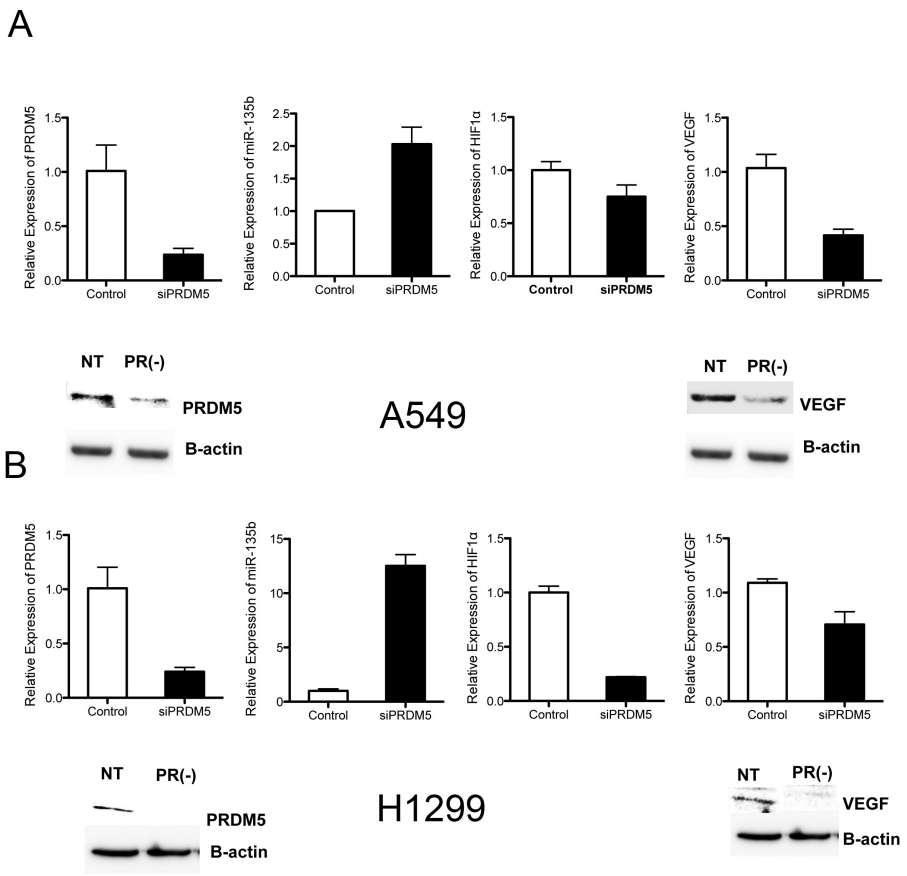

Fig. 8 PRDM5 suppression leads to induction of miR-135b and suppression of HIF1α expression. Quantitative RT-PCR and western blotting showed that inhibition of PRDM5 induce miR-135b which downregulated the expression of HIF1α and VEGF in both cell line A) A549 and B) H1299 cells.

Interaction between PRDM5, miR-135b, HIF1α upon PRDM5 over-expression

In order to further confirm the interaction between PRDM5, miR-135b, and HIF1α, I over-expressed the PRDM5 gene and checked the expression of other candidates. I found that PRDM5 over-expression leads to the suppression of miR-135b and induction of the expression of HIF1α and VEGF respectively at RNA in both A549 (Fig 9A) and H1299 (Fig 9B) cells (VEGF is used as a marker for HIF1α expression).

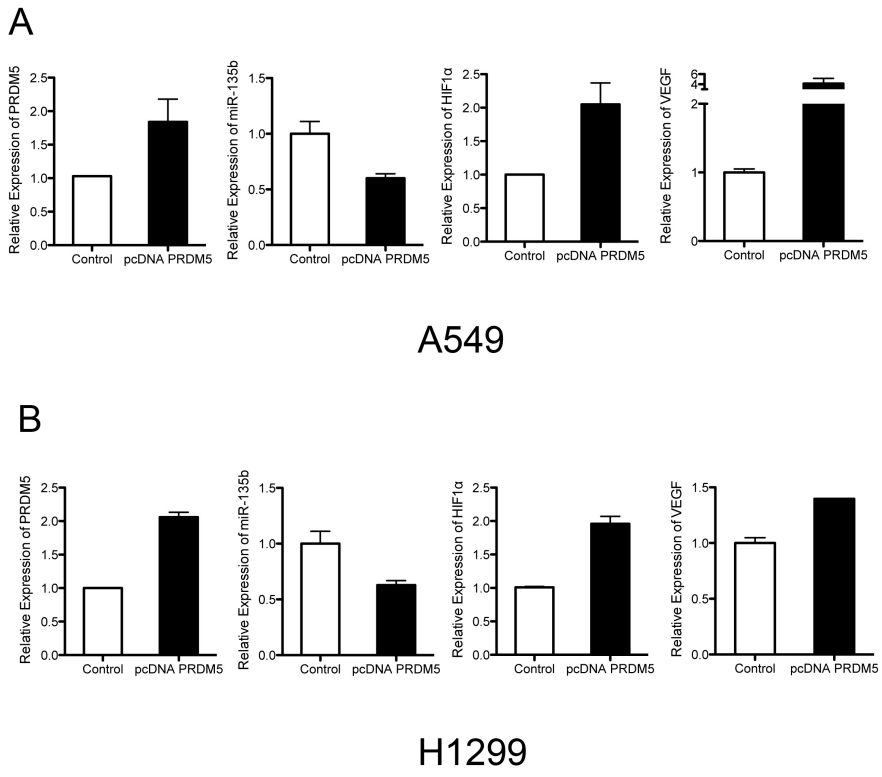

Fig. 9 PRDM5 over-expression leads to suppression of miR-135b and induction of HIF1α expression. Quantitative RT –PCR showing overexpression of PRDM5 reduced the level of miR-135b which causes induction of HIF1α and VEGF in both cell line A) A549 and B) H1299 cells.

Positive correlation of PRDM5 and HIF1α in NSCLC

Enrichment analysis is done considering the GEO datasets [GSE10799, GSE12667, GSE19188, & GSE10245] and interestingly I found that there exists a strong correlation (r=0.5225) between PRDM5 and HIF1α expression in total patients (n=221) samples considered (Fig 10A)(Table 4). Real time PCR (Fig. 10B) and western blot analysis (Fig. 10C) revealed that PRDM5 is positively correlated with HIF1α in NSCLC cell lines.

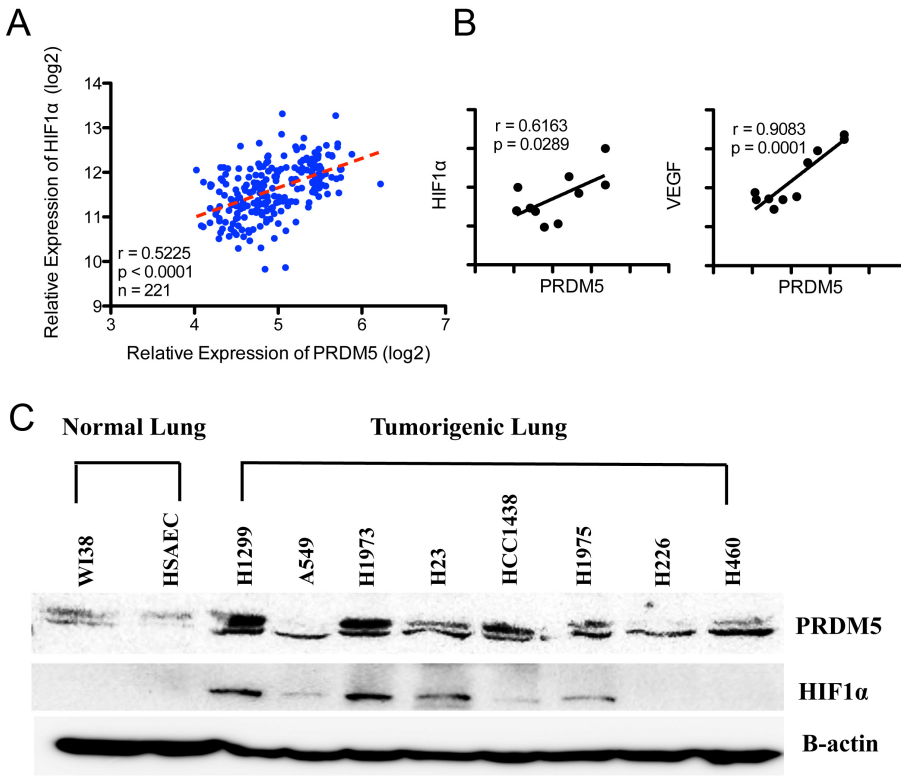

Fig. 10 PRDM5 is correlated to HIF1α and VEGF. A) Enrichment analysis considering GEO datasets [GSE10799, GSE12667, GSE19188, & GSE10245] showing correlation (r=0.5225) between PRDM5 and HIF1α expression in lung cancer patients (n=221) samples. B) Real time PCR revealed that PRDM5 is positively correlated with HIF1α and VEGF in lung cancer cell lines. and C) western blot analysis revealed that PRDM5 is positively correlated with HIF1α in lung cancer cell lines.

miR-135b is Indispensible for PRDM5 mediated regulation

Next, in order to check if miR-135b is indispensable for the PRDM5 regulated mechanism, I co-transfected A549 cells with PRDM5 and miR-135b, and then checked the expression of VEGF. I found that the PRDM5 induced expression of VEGF is suppressed due to the over-expression of miR-135b. Thus indicating that the importance of miR-135b in the PRDM5 mediated regulation (Fig. 11).

Relative Expression of PRDM5, HIF1A and miR-135b in A549 and H1299 cells exposed to ionizing radiation (2Gy)

PRDM5 and HIF1α expression is upregulated when cells were exposed to the 2gy of ionizing radiation and miR-135b expression is down regulated in both A549 and H1299 cell lines (Fig. 12).

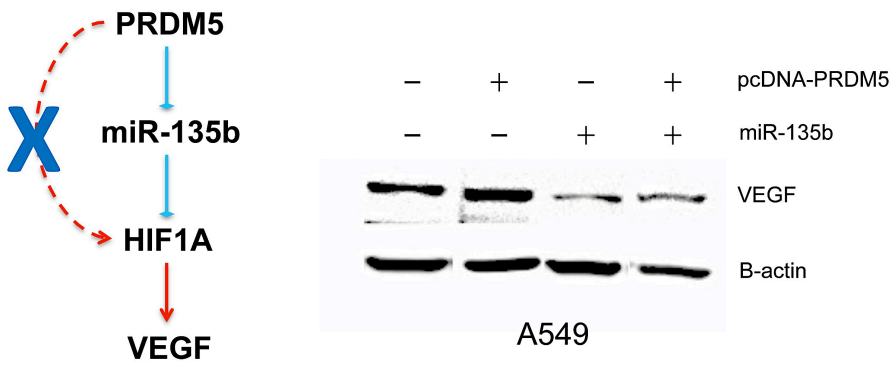

Fig. 11 miR-135b is indispensable for the PRDM5 regulated mechanism. A549 cells co-transfected with PRDM5 and miR-135b. PRDM5 impact on expression of VEGF is checked.

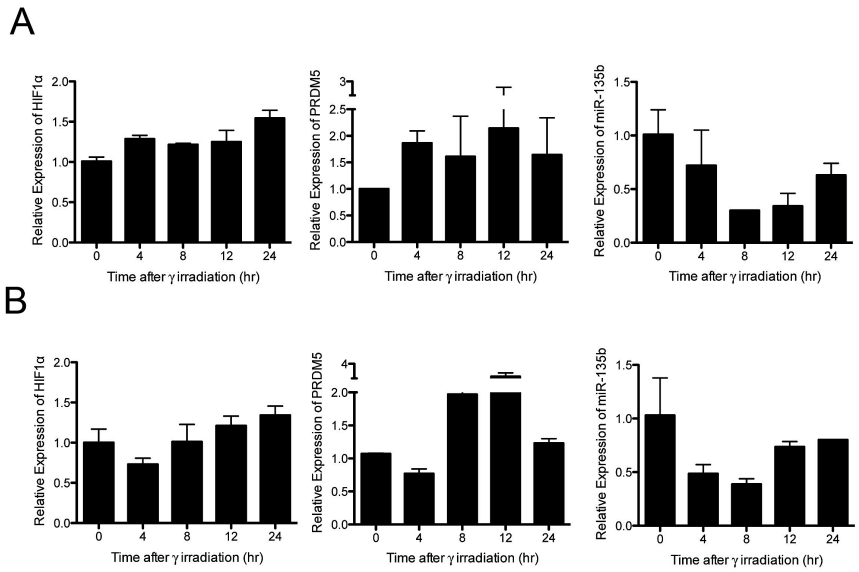

Fig. 12 Impact of Ionizing radiations on PRDM5, miR-135b and HIF1α. Quantitative RT-PCR to show that PRDM5 and HIF1α is induced and miR-135b expression is suppressed when 2Gy of ionizing radiation is given to A) A549 and B) H1299 cell line.

Inhibition of PRDM5 and overexpression of miR-135b leads to radiosensitization

In order to address the effectiveness of PRDM5 in lung cancer cells and to check if PRDM5 is sufficient enough that it could affect the resistance of lung cancer cells upon DNA damage cause by ionizing radiation, A549 & H1299 cells were transfected with siPRDM5, and 48 hours post-transfection, they were exposed to different doses of ionizing radiations. I found that inhibition of PRDM5 lead to the sensitization of both H1299 & A549 cells as measured by MTT assay (Fig. 13A)

In order to check, if this regulation is occurring in other lung cancer cells also I inhibited PRDM5 and checked sensitization in H1573 cells, siPRDM5 sensitized these cells also. From the above experiments I concluded that inhibition of PRDM5 is able to sensitize the H1299, A549 cells and H1573 cell line.

Next in order to find if PRDM5 over-expression could induce resistance in the cancerous cells, I selected H460 cells, which is considered to be a sensitive cell line. First I transfected H460 cells with PRDM5 and 48 hours post transfection I exposed the cells to varying doses of ionizing radiation which leaded to the induction of resistance in H460 cells (Fig 13B).

To address the effectiveness of miR-135b in lung cancer cells and to check if miR-135b is sufficient enough that it could affect the sensitivity of resistance lung cancer cells upon radiations. H1299 & A549 cells were transfected with miR-135b. Over-expression of miR-135b followed by exposure of radio-resistant lung cancer cells to different doses of ionizing radiations led to the sensitization of both H1299 & A549 cells as measured by MTT assay

In order to check, if this regulation is occurring in other lung cancer cells also I over-expressed miR-135b and checked sensitization in H1573 cells, miR-135b sensitized these cells also (Fig 13C).

In conclusion I showed that PRDM5 suppression and miR-135b over-expression leads to the sensitization of resistance lung cancer cells towards ionizing radiations. However when PRDM5 is over-expressed in sensitive lung cancer cells, it leads to the induction of resistance towards the radiations.

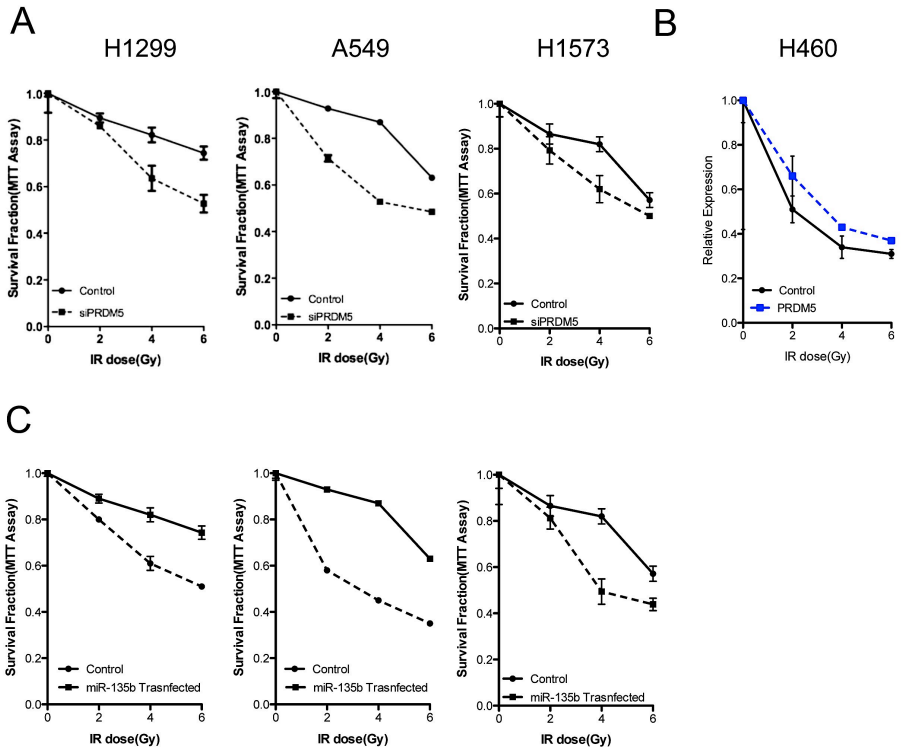

Fig. 13 Suppression of PRDM5 and induction of miR-135b leads to radiosensitization. A) siPRDM5 and siNC were transfected to three cell line H1299, A549 and H1573 and the cell survival fraction upon –y-irradiation was measured using MTT assay. B) PRDM5 overexpressing plasmid was transfected in the H460 (radiosensitive cell line) and the cell survival fraction upon-y- irradiation was measured using MTT assay. C) miR -135b was overexpressed in three cell line (H1299,A549 and H1573) and the cell survival fraction upon –y-irradiation was measured using MTT assays

Drug exposure leads to the induction of PRDM5 and HIF1α

Doxorubicin treatment induced the expression of PRDM5 and HIF1α in both H1299 and A549 cells (Fig 14A). I cloned a PRDM5 promoter region upstream the firefly luciferase coding sequences of the PGL3 –basic plasmid. Promoter constructs were transfected in parallel with a Renilla luciferase-expressing construct (normalizing control). Treat them with .5uM and 1uM of doxorubicin or left untreated for 24hrs.In complete agreement with quantitative PCR experiments doxorubicin treatment was able to activate the promoter activity (Fig 14 B).

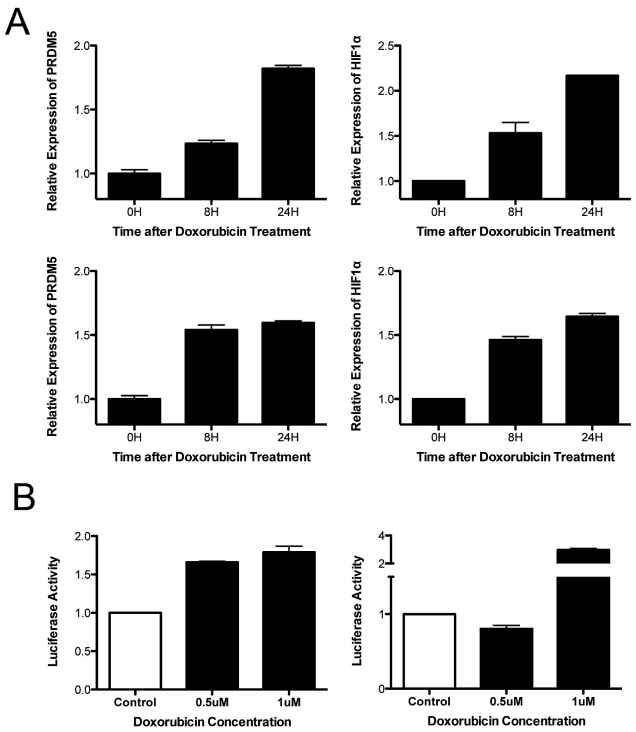

Fig. 14 Doxorubicin induced DNA damage induce PRDM5 expression. A) Quantitative RT- PCR to show PRDM5 is induced when Doxorubicin (10nm) is given to the H1299 and A549 cell line**.** B) PRDM5 promoter reporter constructs cloned in PGL3 basic luciferase reporter plasmid, either expose to the doxorubicin or left untreated for 24 hrs. In all transfection a plasmid expressing, Renilla luciferase was included for normalization.

Suppression of PRDM5 and overexpression of miR-135b leads to the Chemo sensitization

I found that when PRDM5 is inhibited in doxorubicin treated cells it leads to the chemo-sensitization of these cells as compared to the cells, which are treated, with doxorubicin alone. I checked the sensitization at 2.5nM, 5nM and 10nM respectively in A549, H1299 & H1573 cells respectively via MTT assay (Fig. 15A). With colonogenic assay similar result was obtained (Fig. 15B).

I overexpressed the PRDM5 in H460 cell and then exposed them to various concentration of doxorubicin (2.5nM, 5nM and 10nM respectively). I found that PRDM5 over-expression induced resistance in the H460 cells towards doxorubicin (Fig. 15C).

In addition to PRDM5 suppression, I found that when miR-135b is over expressed in doxorubicin treated cells it leads to the chemo-sensitization of these cells as compared to the cells, which are treated, with doxorubicin alone. I checked the sensitization at 2.5nM, 5nM and 10nM respectively in A549, H1299 & H1573 cells respectively via MTT assay (Fig. 16A). With colonogenic assay similar result was obtained (Fig. 16B).

In conclusion I showed that PRDM5 suppression and miR-135b over-expression leads to the sensitization of resistance lung cancer cells towards doxorubicin treatment. However when PRDM5 is over-expressed in sensitive lung cancer cells, it leads to the induction of resistance towards the radiations (Fig. 16C).

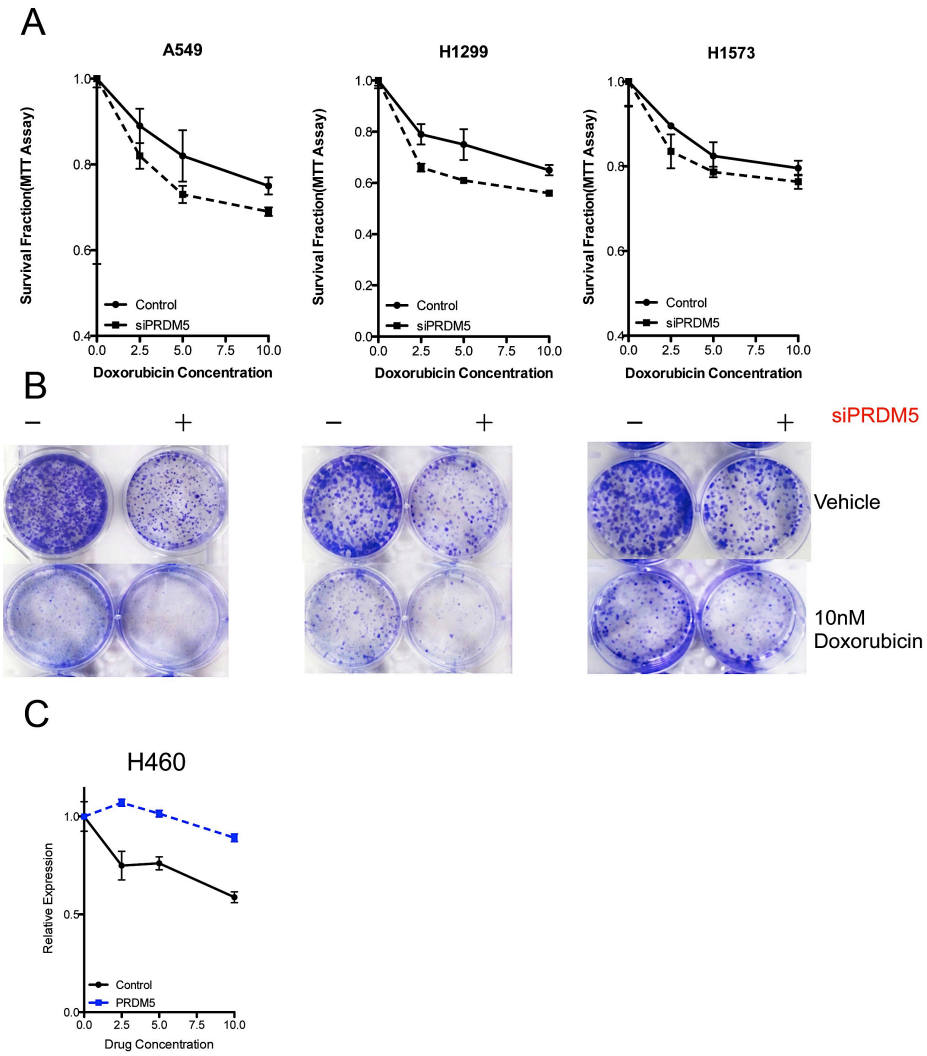

Fig. 15 PRDM5 impact on chemo-sensitization. siPRDM5 and siNC were transfected to the three cell line A549, H1299 and H1573 and the cell fraction upon treatment with different doses of doxorubicin (nM) was measured using A) MTT assay**.** B) clonogenic assay showing

siPRDM5 leads to the chemo sensitization C) PRDM5 overexpressing plasmid was transfected in the H460 and the cell fraction upon treatment with different doses of doxorubicin (nM) was measured using MTT assay.

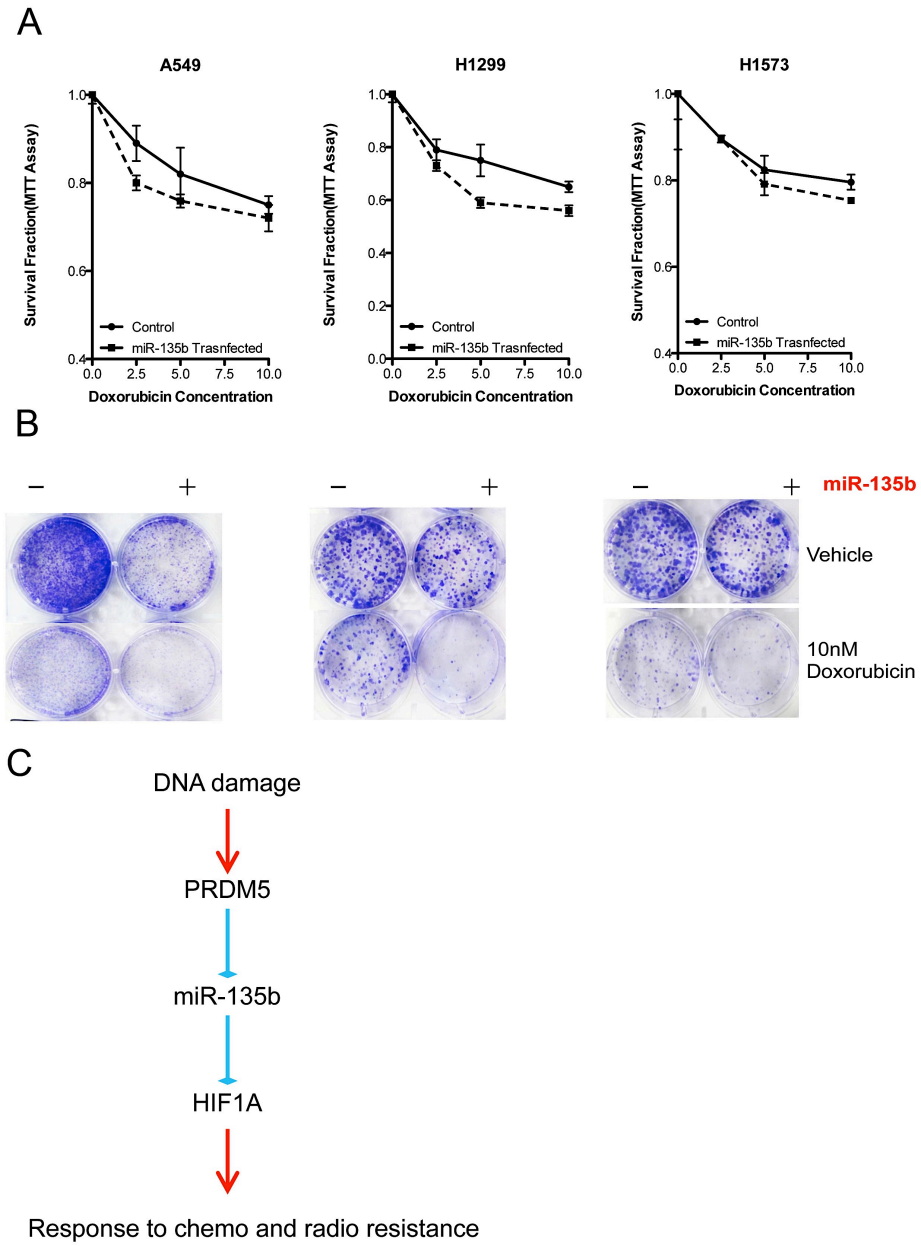
A
A549
H1299
H1573
Survival Fraction(MTT Assay)
Control
miR-135b Trasnfected
Doxorubicin Concentration
B
miR-135b
Vehicle
10nM
Doxorubicin
C
DNA damage
PRDM5
miR-135b
HIF1A
Response to chemo and radio resistance

Fig. 16 Impact of miR-135b on chemo-sensitization. miR-135b was overexpressed in three cell line A549, H1299 and H1573 and the cell survival fraction upon treatment with different doses of doxorubicin (nM) was measured using A) MTT assay. B) Clonogenic assay showing miR-135b overexpression leads to chemo sensitization. C) Conclusive figure.

DISCUSSION

Non–small-cell lung carcinoma (NSCLC) represents approximately 80% of lung cancers and has a 5-year survival rate of only 16% (Albano, Ward et al. 2007). Early-stage (stage I and II) patients are treated primarily by surgical resection. However, 30% to 55% of these patients develop recurrence and die of the disease (Mountain 1985; Naruke, Goya et al. 1988).

In this study I showed that PRDM5 is highly expressed in the NSCLC lung cancer cell lines when compared to the normal cell lines. When PRDM5 is inhibited it reduces the growth of NSCLC lung cancer cell lines. PRDM5 binds to the promoter region of miR135b and regulates its expression in a inverse manner. miR-135b, directly targets the 3'UTR of HIF1α and thereby further regulating VEGF, a downstream member to HIF1α. I find out that miR-135b is down regulated in the NSCLCs, when miR-135b is over-expressed it inhibited the growth of NSCLCs by inhibiting HIF1α and VEGF respectively.

Analysis of regulatory elements of the PRDM5 promoter by TFSearch (www.cbrc.jp/research/db/TFSEARCH) revealed two HSF (heat shock factor) and five Sp1 binding sites, suggesting the role of PRDM5 as a stress -responsive gene (Shu, Geng et al. 2011). I found that when DNA damage is induced in NSCLCs by either Ionizing radiation or Doxorubicin, PRDM5 is induced, which further down-regulated the expression of miR-135b, as a result of which HIF1α is induced, which

induces resistant toward drug and ionizing radiation .I also showed that when PRDM5 is inhibited, it lead to radio sensitization and chemo sensitization of resistant NSCLC's. Interestingly, when the PRDM5 is over-expressed, the radiosensitive cell become resistant toward radiations and drug. My finding supports the role of PRDM5 as stress responsive gene.

Blocking of HIF-1 significantly increased tumor radio-sensitivity by enhancing vascular destruction (Moeller, Cao et al. 2004; Moeller and Dewhirst 2004). Over-expression of HIF-1α in tumor biopsy samples has been associated with a poor response to radiotherapy in multiple cancer types (Aebersold 2006). In this finding I found that inhibition of PRDM5 leads to the inhibition of the HIF1α and it also down-regulate the expression of VEGF, which could be a major cause of resistance. Similarly, when I over-expressed miR-135b, it also leads to the radio-sensitization for the similar reasons. In other set of experiment I have also shown when I over-express the PRDM5 in a radiosensitive cells, the cell become resistant toward the treatment. From this study I conclude that down-regulation of PRDM5 can leads to the radio-sensitization.

Genetic approaches and small-molecule inhibitors targeting HIF1α have proven effective at decreasing hypoxia-induced resistance to chemotherapeutics non–small cell lung cancer cells (Han, Lee et al. 2006; Park, Song et al. 2007), thereby highlighting the importance of HIF-1 in the acquisition of drug resistance. I found in my study that

when PRDM5 expression is inhibited, the NSCLCs become sensitive for the drug similarly like the radio-sensitization. Similarly when I over-express miR-135b, the NSCLCs become sensitive to the drug. PRDM5 over-expression makes the cells more resistant towards the drug

This is to my knowledge, the first large scale study of PRDM5 in NSCLC lung cancer patient. Here for the first time I are reporting that PRDM5 is highly expressed in 53.8% of the NSCLC lung patient. In addition to this, I found that PRDM5 and HIF1α are positively correlated in NSCLC lung cancer patient. I have also shown the clinical association of PRDM5 expression with the poor Relapse free survival. In support of the clinical association, a survey across different NSCLC lung cancer cell lines revealed a high expression of PRDM5. I have also deduced a molecular mechanism by which the resistance is developed in the patients.

Table 1. candidates for Survival Analysis

ID_REF	PRDM5 [log2]	Cell type	Surv (months)	STATUS	GEO ID	PUBMED ID	Platform
GSM70221	9.958842675	SCC	10.5	1	GSE3141	16273092	HG-U133_Plus_2
GSM70202	9.774292901	SCC	23.63333333	1	GSE3141	16273092	HG-U133_Plus_2
GSM70180	9.682292371	SCC	55.93333333	0	GSE3141	16273092	HG-U133_Plus_2
GSM70168	9.602698865	SCC	9.533333333	1	GSE3141	16273092	HG-U133_Plus_2
GSM70132	9.576106381	SCC	5.166666667	0	GSE3141	16273092	HG-U133_Plus_2
GSM70142	9.552861188	SCC	28.1	1	GSE3141	16273092	HG-U133_Plus_2
GSM70231	9.534497434	SCC	6	1	GSE3141	16273092	HG-U133_Plus_2
GSM70152	9.470252137	SCC	48.63333333	0	GSE3141	16273092	HG-U133_Plus_2
GSM70178	9.445014846	SCC	9.733333333	1	GSE3141	16273092	HG-U133_Plus_2
GSM70147	9.430034319	SCC	39.26666667	1	GSE3141	16273092	HG-U133_Plus_2
GSM70149	9.316734071	SCC	31.9	1	GSE3141	16273092	HG-U133_Plus_2
GSM70228	9.301953395	SCC	34	1	GSE3141	16273092	HG-U133_Plus_2
GSM70158	9.29530977	SCC	5.3	1	GSE3141	16273092	HG-U133_Plus_2
GSM70200	9.237926947	SCC	13.26666667	1	GSE3141	16273092	HG-U133_Plus_2
GSM70135	9.22905912	SCC	71.1	0	GSE3141	16273092	HG-U133_Plus_2
GSM70137	9.209453366	SCC	17	1	GSE3141	16273092	HG-U133_Plus_2
GSM70182	9.207502459	SCC	28.86666667	1	GSE3141	16273092	HG-U133_Plus_2
GSM70207	9.201633861	SCC	2.633333333	0	GSE3141	16273092	HG-U133_Plus_2
GSM70176	9.189824559	SCC	43.8	0	GSE3141	16273092	HG-U133_Plus_2
GSM70215	9.109047078	SCC	39.6	1	GSE3141	16273092	HG-U133_Plus_2
GSM70211	9.038644687	SCC	25.53333333	0	GSE3141	16273092	HG-U133_Plus_2
GSM70160	9.032596795	SCC	59.4	0	GSE3141	16273092	HG-U133_Plus_2
GSM70162	8.954487147	SCC	14.13333333	1	GSE3141	16273092	HG-U133_Plus_2
GSM70146	8.931032942	SCC	8.666666667	1	GSE3141	16273092	HG-U133_Plus_2
GSM136000	1.5145181	ADC	70.51	0	GSE5843	18556351	MG_U74A/B/Cv2
GSM136021	1.2521436	ADC	15.44	1	GSE5843	18556351	MG_U74A/B/Cv2
GSM136020	1.1333069	ADC	14.03	1	GSE5843	18556351	MG_U74A/B/Cv2
GSM136026	1.0927311	ADC	25.82	1	GSE5843	18556351	MG_U74A/B/Cv2
GSM136016	1.0178652	ADC	4.21	1	GSE5843	18556351	MG_U74A/B/Cv2
GSM135997	0.8847406	ADC	69.82	0	GSE5843	18556351	MG_U74A/B/Cv2
GSM136023	0.8175302	ADC	26.48	1	GSE5843	18556351	MG_U74A/B/Cv2
GSM136030	0.7757221	ADC	11.43	1	GSE5843	18556351	MG_U74A/B/Cv2
GSM135990	0.72132736	ADC	132.93	0	GSE5843	18556351	MG_U74A/B/Cv2

GSM136001	0.7098509	ADC	57.89	0	GSE5843	18556351	MG_U74A/B/Cv2
GSM136019	0.6985395	ADC	14.23	1	GSE5843	18556351	MG_U74A/B/Cv2
GSM136024	0.59749013	ADC	26.18	1	GSE5843	18556351	MG_U74A/B/Cv2
GSM136013	0.56908464	ADC	54.67	1	GSE5843	18556351	MG_U74A/B/Cv2
GSM135996	0.5495637	ADC	70.57	0	GSE5843	18556351	MG_U74A/B/Cv2
GSM136028	0.54565626	ADC	12.88	1	GSE5843	18556351	MG_U74A/B/Cv2
GSM136005	0.5144075	ADC	50.79	0	GSE5843	18556351	MG_U74A/B/Cv2
GSM136027	0.5091795	ADC	8.21	1	GSE5843	18556351	MG_U74A/B/Cv2
GSM136002	0.5068356	ADC	56.11	1	GSE5843	18556351	MG_U74A/B/Cv2
GSM135987	0.49717814	ADC	154.87	0	GSE5843	18556351	MG_U74A/B/Cv2
GSM135999	0.47059983	ADC	67.25	0	GSE5843	18556351	MG_U74A/B/Cv2
GSM136003	0.40391687	ADC	54.47	0	GSE5843	18556351	MG_U74A/B/Cv2
GSM136029	0.2915166	ADC	27.1	1	GSE5843	18556351	MG_U74A/B/Cv2
GSM136014	0.27946317	ADC	7.92	1	GSE5843	18556351	MG_U74A/B/Cv2
GSM70192	8.764871591	SCC	74.63333333	0	GSE3141	16273092	HG-U133_Plus_2
GSM70187	8.763212367	SCC	12.33333333	1	GSE3141	16273092	HG-U133_Plus_2
GSM70133	8.729960561	SCC	35.1	0	GSE3141	16273092	HG-U133_Plus_2
GSM70230	8.701826258	SCC	>72	0	GSE3141	16273092	HG-U133_Plus_2
GSM70166	8.570614722	SCC	6.333333333	1	GSE3141	16273092	HG-U133_Plus_2
GSM70198	8.548051238	SCC	33.8	1	GSE3141	16273092	HG-U133_Plus_2
GSM70141	8.541096615	SCC	13.1	1	GSE3141	16273092	HG-U133_Plus_2
GSM70157	8.517669388	SCC	22.5	1	GSE3141	16273092	HG-U133_Plus_2
GSM70143	8.505017556	SCC	87.26666667	0	GSE3141	16273092	HG-U133_Plus_2
GSM70139	8.50422312	SCC	68.36666667	0	GSE3141	16273092	HG-U133_Plus_2
GSM70216	8.474517164	SCC	64	0	GSE3141	16273092	HG-U133_Plus_2
GSM70188	8.471675214	SCC	33.43333333	0	GSE3141	16273092	HG-U133_Plus_2
GSM70206	8.442114122	SCC	36.16666667	0	GSE3141	16273092	HG-U133_Plus_2
GSM70205	8.377644358	SCC	31.13333333	0	GSE3141	16273092	HG-U133_Plus_2
GSM70134	8.37286506	SCC	14.46666667	1	GSE3141	16273092	HG-U133_Plus_2
GSM70185	8.238882374	SCC	51.26666667	1	GSE3141	16273092	HG-U133_Plus_2
GSM70217	8.029011087	SCC	60	0	GSE3141	16273092	HG-U133_Plus_2
GSM70167	7.891783703	SCC	45.26666667	1	GSE3141	16273092	HG-U133_Plus_2
GSM70232	7.871597266	SCC	21	1	GSE3141	16273092	HG-U133_Plus_2
GSM70189	7.825912799	SCC	59.23333333	0	GSE3141	16273092	HG-U133_Plus_2
GSM70212	7.692092375	SCC	25.43333333	0	GSE3141	16273092	HG-U133_Plus_2
GSM70210	7.648177796	SCC	2.733333333	0	GSE3141	16273092	HG-U133_Plus_2

GSM70125	7.479780264	SCC	57.83333333	0	GSE3141	16273092	HG-U133_Plus_2
GSM70213	6.768184325	SCC	31.13333333	1	GSE3141	16273092	HG-U133_Plus_2
GSM70191	5.714245518	SCC	82.93333333	0	GSE3141	16273092	HG-U133_Plus_2
GSM70126	5.057450272	SCC	66.03333333	0	GSE3141	16273092	HG-U133_Plus_2
GSM70128	4.958842675	SCC	13.96666667	0	GSE3141	16273092	HG-U133_Plus_2
GSM136031	0.2756001	ADC	33.54	0	GSE5843	18556351	MG_U74A/B/Cv2
GSM135985	0.20531285	ADC	168.87	0	GSE5843	18556351	MG_U74A/B/Cv2
GSM136004	0.19916092	ADC	53.06	0	GSE5843	18556351	MG_U74A/B/Cv2
GSM136007	0.19530058	ADC	46.03	0	GSE5843	18556351	MG_U74A/B/Cv2
GSM136018	0.19193776	ADC	13.5	1	GSE5843	18556351	MG_U74A/B/Cv2
GSM135992	0.1870124	ADC	69.22	0	GSE5843	18556351	MG_U74A/B/Cv2
GSM135994	0.17535768	ADC	92.52	0	GSE5843	18556351	MG_U74A/B/Cv2
GSM135991	0.117250524	ADC	83.35	1	GSE5843	18556351	MG_U74A/B/Cv2
GSM136015	0.02925732	ADC	24.64	1	GSE5843	18556351	MG_U74A/B/Cv2
GSM136011	0.013424978	ADC	24.34	1	GSE5843	18556351	MG_U74A/B/Cv2
GSM136010	-0.030608712	ADC	6.57	1	GSE5843	18556351	MG_U74A/B/Cv2
GSM136006	-0.10705436	ADC	53.4	0	GSE5843	18556351	MG_U74A/B/Cv2
GSM135983	-0.12905326	ADC	124.81	0	GSE5843	18556351	MG_U74A/B/Cv2
GSM136022	-0.15369473	ADC	64.36	0	GSE5843	18556351	MG_U74A/B/Cv2
GSM135988	-0.20430322	ADC	148.34	0	GSE5843	18556351	MG_U74A/B/Cv2
GSM136017	-0.214988	ADC	30.32	1	GSE5843	18556351	MG_U74A/B/Cv2
GSM135993	-0.29144615	ADC	113.68	0	GSE5843	18556351	MG_U74A/B/Cv2
GSM136009	-0.41518793	ADC	164.04	0	GSE5843	18556351	MG_U74A/B/Cv2
GSM135995	-0.42355415	ADC	70.44	0	GSE5843	18556351	MG_U74A/B/Cv2
GSM135998	-0.47031617	ADC	66.56	0	GSE5843	18556351	MG_U74A/B/Cv2
GSM135984	-0.6335118	ADC	124.12	1	GSE5843	18556351	MG_U74A/B/Cv2
GSM136025	-0.65559965	ADC	24.74	1	GSE5843	18556351	MG_U74A/B/Cv2
GSM136008	-0.7047028	ADC	44.39	0	GSE5843	18556351	MG_U74A/B/Cv2
GSM135986		ADC	184.11	0	GSE5843	18556351	MG_U74A/B/Cv2
GSM136012		ADC	21.82	1	GSE5843	18556351	MG_U74A/B/Cv2

Table 2 Correlation analysis between HIF1α and miR-135b in NCI60 cell lines

cell line	HIF1α	GEO-ID	PUBMED ID	miR-135b	GEO-ID	PUBMED ID
786-0	12.27151386	GSE32474	19584232	7.219313249	GSE26375	21252286
A498	10.14805341	GSE32474	19584232	6.891701913	GSE26375	21252286
A549	11.45609236	GSE32474	19584232	6.732587	GSE26375	21252286
ACHN	11.82659977	GSE32474	19584232	7.204948448	GSE26375	21252286
BT-549	9.539660726	GSE32474	19584232	9.085979866	GSE26375	21252286
CAKI-1	11.98040044	GSE32474	19584232	6.72457227	GSE26375	21252286
CCRF-CEM	10.46581761	GSE32474	19584232	6.415823262	GSE26375	21252286
COLO 205	3.324330302	GSE32474	19584232	9.71664397	GSE26375	21252286
DU-145	11.42849629	GSE32474	19584232	7.909983352	GSE26375	21252286
EKVX	10.18992071	GSE32474	19584232	6.993052642	GSE26375	21252286
HCC-2998	11.93923031	GSE32474	19584232	8.630998063	GSE26375	21252286
HCT-116	11.53417834	GSE32474	19584232	8.315214294	GSE26375	21252286
HCT-15	12.79382513	GSE32474	19584232	7.022093154	GSE26375	21252286
HL-60	11.79825152	GSE32474	19584232	6.514848516	GSE26375	21252286
HOP-62	10.64141053	GSE32474	19584232	6.740672314	GSE26375	21252286
HOP-92	11.01941358	GSE32474	19584232	7.524779318	GSE26375	21252286
HS 578T	9.865473103	GSE32474	19584232	6.587126659	GSE26375	21252286
HT29	11.88790454	GSE32474	19584232	8.56071795	GSE26375	21252286
IGROV1	11.10458812	GSE32474	19584232	8.322022669	GSE26375	21252286
K-562	10.70726436	GSE32474	19584232	6.927432861	GSE26375	21252286
KM12	11.2199072	GSE32474	19584232	7.39056491	GSE26375	21252286
LOX IMVI	9.063193992	GSE32474	19584232	6.597493602	GSE26375	21252286
M14	11.74670936	GSE32474	19584232	7.920875741	GSE26375	21252286
MALME-3M	10.77607088	GSE32474	19584232	6.96900511	GSE26375	21252286
MCF7	10.79326013	GSE32474	19584232	7.963329846	GSE26375	21252286
MDA-MB-231	11.61819072	GSE32474	19584232	6.935887766	GSE26375	21252286
MDA-MB-435	10.03955545	GSE32474	19584232	6.785025012	GSE26375	21252286
MOLT-4	12.59278528	GSE32474	19584232	6.513136092	GSE26375	21252286

NCI/ADR-RES	10.40624661	GSE32474	19584232	6.748220615	GSE26375	21252286
NCI-H226	12.08747036	GSE32474	19584232	7.02330474	GSE26375	21252286
NCI-H23	11.74602713	GSE32474	19584232	6.869953073	GSE26375	21252286
NCI-H322M	11.87303189	GSE32474	19584232	9.6849935	GSE26375	21252286
NCI-H460	12.413444	GSE32474	19584232	6.588592709	GSE26375	21252286
NCI-H522	9.316593457	GSE32474	19584232	6.567188223	GSE26375	21252286
OVCAR-3	10.65080477	GSE32474	19584232	8.963754964	GSE26375	21252286
OVCAR-4	11.86292402	GSE32474	19584232	8.055209215	GSE26375	21252286
OVCAR-5	10.58911712	GSE32474	19584232	8.904415723	GSE26375	21252286
OVCAR-8	12.07942434	GSE32474	19584232	6.974644389	GSE26375	21252286
PC-3	11.1282142	GSE32474	19584232	7.155527003	GSE26375	21252286
RPMI-8226	11.61120168	GSE32474	19584232	6.47569617	GSE26375	21252286
RXF 393	11.75525848	GSE32474	19584232	6.751178492	GSE26375	21252286
SF-268	11.68671793	GSE32474	19584232	6.608104929	GSE26375	21252286
SF-295	11.67431395	GSE32474	19584232	7.046043209	GSE26375	21252286
SF-539	12.48368519	GSE32474	19584232	6.654690112	GSE26375	21252286
SK-MEL-2	11.19596702	GSE32474	19584232	7.143325274	GSE26375	21252286
SK-MEL-28	11.06109573	GSE32474	19584232	6.694344218	GSE26375	21252286
SK-MEL-5	11.59658091	GSE32474	19584232	8.743732147	GSE26375	21252286
SK-OV-3	10.62619625	GSE32474	19584232	7.291002815	GSE26375	21252286
SN12C	10.45982318	GSE32474	19584232	7.313402288	GSE26375	21252286
SNB-19	11.38966922	GSE32474	19584232	7.603730384	GSE26375	21252286
SNB-75	11.57325527	GSE32474	19584232	6.886739519	GSE26375	21252286
SR	10.6768521	GSE32474	19584232	7.308363123	GSE26375	21252286
SW-620	12.32294429	GSE32474	19584232	9.226676587	GSE26375	21252286
T-47D	9.57695377	GSE32474	19584232	6.630370194	GSE26375	21252286
TK-10	12.09782505	GSE32474	19584232	6.67681637	GSE26375	21252286
U251	11.27896744	GSE32474	19584232	8.827873808	GSE26375	21252286
UACC-257	12.1682425	GSE32474	19584232	6.732403284	GSE26375	21252286
UACC-62	11.93480542	GSE32474	19584232	6.854517263	GSE26375	21252286
UO-31	11.72991783	GSE32474	19584232	7.525767551	GSE26375	21252286

Table 3. List of primers used in the study

Name	Sequences of primers used in the study 5'-3'.
PRDM5 CDS Forward Primer	GAAAATGCTGGGCATGTACG
PRDM5 CDS REVERSE Primer	CCAGTAAGTCACTTTTGGCTACTTC
HIF1 3 UTR Forward	AATTCTCGAGGTGGTAGCCACAATTGCACA
HIF1 3 UTR Reverse	AATTGCGGCCGCCTTTTGAGCTGGCAAAGTGA
HIF 1QRT Forward	GCTGGATCACAGACAGCTCA
HIF1 QRT Reverse	GGGATAAACTCCCTAGCCAAA
VEGF QRT forward	CCTGAAATGAAGGAAGAGGAGA
VEGF QRT Reverse	GGCGAATCCAATTCCAAGAG
PRDM5 QRT forward	CTTCTCCCTTACTCCCACGA
PRDM5 QRT Reverse	AAGGGTGAAAAGTTCGGACC
PRDM5 promoter Primer Forward	AATTCTCGAGGCATAACTCAAATGTGAGAAGCA
PRDM5 promoter Primer Reverse	AATTAAGCTTATCCGTTCCTGCCATTCC

REFERENCE

Aebersold, D. M. (2006). "[Radiotherapy of the prostate gland--old wine in a new bottle?]." Ther Umsch **63**(2): 151-156.

Albano, J. D., E. Ward, et al. (2007). "Cancer mortality in the United States by education level and race." J Natl Cancer Inst **99**(18): 1384-1394.

Araki, T. and J. Milbrandt (1996). "Ninjurin, a novel adhesion molecule, is induced by nerve injury and promotes axonal growth." Neuron **17**(2): 353-361.

Arora, H., R. Qureshi, et al. (2011). "miR-9 and let-7g enhance the sensitivity to ionizing radiation by suppression of NFkappaB1." Experimental & molecular medicine **43**(5): 298-304.

Bartel, D. P. (2004). "MiRNAs: genomics, biogenesis, mechanism, and function." Cell **116**(2): 281-297.

Bartel, D. P. (2009). "MiRNAs: target recognition and regulatory functions." Cell **136**(2): 215-233.

Belaiba, R. S., S. Bonello, et al. (2007). "Hypoxia up-regulates hypoxia-inducible factor-1alpha transcription by involving phosphatidylinositol 3-kinase and nuclear factor kappaB in pulmonary artery smooth muscle cells." Molecular biology of the cell **18**(12): 4691-4697.

Brennecke, J., D. R. Hipfner, et al. (2003). "bantam encodes a developmentally regulated miRNA that controls cell proliferation and regulates the proapoptotic gene hid in Drosophila." Cell **113**(1): 25-36.

Chang, C. J., C. H. Chao, et al. (2011). "p53 regulates epithelial-mesenchymal transition and stem cell properties through modulating miRNAs." Nat Cell Biol **13**(3): 317-323.

Chang, T. C., D. Yu, et al. (2008). "Widespread miRNA repression by Myc contributes to tumorigenesis." Nature genetics **40**(1): 43-50.

Chen, Y., J. Zuo, et al. (2010). "Inhibitory effects of miRNA-200c on chemotherapy-resistance and cell proliferation of gastric cancer SGC7901/DDP cells." Chinese journal of cancer **29**(12): 1006-1011.

Deng, Q. and S. Huang (2004). "PRDM5 is silenced in human cancers and has growth suppressive activities." Oncogene **23**(28): 4903-4910.

Duan, Z., R. E. Person, et al. (2007). "Epigenetic regulation of protein-coding and miRNA genes by the Gfi1-interacting tumor suppressor PRDM5." Molecular and cellular biology **27**(19): 6889-6902.

Gessert, S., V. Bugner, et al. (2010). "FMR1/FXR1 and the miRNA pathway are required for eye and neural crest development." Dev Biol **341**(1): 222-235.

Gibson, M. A., D. I. Leavesley, et al. (1999). "Microfibril-associated glycoprotein-2 specifically interacts with a range of bovine and human cell types via alphaVbeta3 integrin." The Journal of biological chemistry **274**(19): 13060-13065.

Han, H. D., A. Lee, et al. (2006). "In vivo distribution and antitumor activity of heparin-stabilized doxorubicin-loaded liposomes." Int J Pharm **313**(1-2): 181-188.

Harada, H., S. Itasaka, et al. (2009). "Treatment regimen determines whether an HIF-1 inhibitor enhances or inhibits the effect of radiation therapy." British journal of cancer **100**(5): 747-757.

Hatziapostolou, M. and D. Iliopoulos (2011). "Epigenetic aberrations during oncogenesis." Cellular and molecular life sciences : CMLS **68**(10): 1681-1702.

Jeong, S. H., H. G. Wu, et al. (2009). "LIN28B confers radio-resistance through the posttranscriptional control of KRAS." Experimental & molecular medicine **41**(12): 912-918.

Kent, O. A. and J. T. Mendell (2006). "A small piece in the cancer puzzle: miRNAs as tumor suppressors and oncogenes." Oncogene **25**(46): 6188-6196.

Marson, A., S. S. Levine, et al. (2008). "Connecting miRNA genes to the core transcriptional regulatory circuitry of embryonic stem cells." Cell **134**(3): 521-533.

Meani, N., F. Pezzimenti, et al. (2009). "The tumor suppressor PRDM5 regulates Wnt signaling at early stages of zebrafish development." PloS one **4**(1): e4273.

Moeller, B. J., Y. Cao, et al. (2004). "Radiation activates HIF-1 to regulate vascular radiosensitivity in tumors: role of reoxygenation, free radicals, and stress granules." Cancer cell **5**(5): 429-441.

Moeller, B. J. and M. W. Dewhirst (2004). "Raising the bar: how HIF-1 helps determine tumor radiosensitivity." Cell Cycle **3**(9): 1107-1110.

Mountain, C. F. (1985). "The biological operability of stage III non-small cell lung cancer." Ann Thorac Surg **40**(1): 60-64.

Nam, S. Y., Y. S. Ko, et al. (2011). "A hypoxia-dependent upregulation of hypoxia-inducible factor-1 by nuclear factor-kappaB promotes gastric tum HIF1α growth and angiogenesis." British journal of cancer **104**(1): 166-174.

Naruke, T., T. Goya, et al. (1988). "The importance of surgery to non-small cell carcinoma of lung with mediastinal lymph node metastasis." Ann Thorac Surg **46**(6): 603-610.

Oliveras-Ferraros, C., S. Cufi, et al. (2011). "Micro(mi)RNA expression profile of breast cancer epithelial cells treated with the anti-diabetic drug metformin: induction of the tumor suppressor miRNA let-7a and suppression of the TGFbeta-induced oncomiR miRNA-181a." Cell Cycle **10**(7): 1144-1151.

Ormestad, M., J. Astorga, et al. (2006). "Foxf1 and Foxf2 control murine gut development by limiting mesenchymal Wnt signaling and

promoting extracellular matrix production." Development **133**(5): 833-843.

Park, S. E., J. D. Song, et al. (2007). "Diphenyleneiodonium induces ROS-independent p53 expression and apoptosis in human RPE cells." FEBS Lett **581**(2): 180-186.

Poliak, S., L. Gollan, et al. (1999). "Caspr2, a new member of the neurexin superfamily, is localized at the juxtaparanodes of myelinated axons and associates with K+ channels." Neuron **24**(4): 1037-1047.

Schanen, B. C. and X. Li (2011). "Transcriptional regulation of mammalian miRNA genes." Genomics **97**(1): 1-6.

Schneider, R., A. J. Bannister, et al. (2002). "Unsafe SETs: histone lysine methyltransferases and cancer." Trends Biochem Sci **27**(8): 396-402.

Semenza, G. L. (2004). "Intratumoral hypoxia, radiation resistance, and HIF-1." Cancer cell **5**(5): 405-406.

Shin, S., H. J. Cha, et al. (2009). "Alteration of miRNA profiles by ionizing radiation in A549 human non-small cell lung cancer cells." International journal of oncology **35**(1): 81-86.

Shu, X. S., H. Geng, et al. (2011). "The epigenetic modifier PRDM5 functions as a tumor suppressor through modulating WNT/beta-catenin signaling and is frequently silenced in multiple tumors." PloS one **6**(11): e27346.

Simone, N. L., B. P. Soule, et al. (2009). "Ionizing radiation-induced oxidative stress alters miRNA expression." PloS one **4**(7): e6377.

Timpl, R., T. Sasaki, et al. (2003). "Fibulins: a versatile family of extracellular matrix proteins." Nat Rev Mol Cell Biol **4**(6): 479-489.

Watanabe, Y., M. Toyota, et al. (2007). "PRDM5 identified as a target of epigenetic silencing in colorectal and gastric cancer." Clinical cancer research : an official journal of the American Association for Cancer Research **13**(16): 4786-4794.

Weidhaas, J. B., I. Babar, et al. (2007). "MiRNAs as potential agents to alter resistance to cytotoxic anticancer therapy." Cancer Res **67**(23): 11111-11116.

Xi, Y., R. Shalgi, et al. (2006). "Differentially regulated micro-RNAs and actively translated messenger RNA transcripts by tumor suppressor p53 in colon cancer." Clinical cancer research : an official journal of the American Association for Cancer Research **12**(7 Pt 1): 2014-2024.

Yamakuchi, M., C. D. Lotterman, et al. (2010). "P53-induced miRNA-107 inhibits HIF-1 and tumor angiogenesis." Proc Natl Acad Sci U S A **107**(14): 6334-6339.

Zhang, H. L., L. F. Yang, et al. (2011). "Serum miRNA-21: elevated levels in patients with metastatic hormone-refractory prostate cancer and potential predictive factor for the efficacy of docetaxel-based chemotherapy." The Prostate **71**(3): 326-331.

Zhou, Y., J. Ferguson, et al. (2007). "Inter- and intra-combinatorial regulation by transcription factors and miRNAs." BMC Genomics **8**: 396.